

# **ACCURACY OF DTM DERIVED FROM UAV IMAGERY AND ITS EFFECT ON CANOPY HEIGHT MODEL COMPARED TO AIRBORNE LIDAR IN PART OF TROPICAL RAIN FORESTS OF BERKLAH, MALAYSIA**

SOLOMON BEGASHAW

Enschede, The Netherlands, February, 2018

SUPERVISORS:


Dr. Y. A. Hussin

Drs. E. H. Kloosterman

ADVISOR:

Dr. Zulkiflee Abd Latif





# ACCURACY OF DTM DERIVED FROM UAV IMAGERY AND ITS EFFECT ON CANOPY HEIGHT MODEL COMPARED TO AIRBORNE LIDAR IN PART OF TROPICAL RAIN FORESTS OF BERKLAH, MALAYSIA

SOLOMON BEGASHAW

Enschede, The Netherlands, February, 2018

Thesis submitted to the Faculty of Geo-Information Science and Earth Observation of the University of Twente in partial fulfilment of the requirements for the degree of Master of Science in Geo-information Science and Earth Observation.  
Specialization: Natural Resource management

**SUPERVISORS:**

Dr. Y. A. Hussin  
Drs. E. H. Kloosterman

**ADVISOR:**

Dr. Zulkiflee Abd Latif

**THESIS ASSESSMENT BOARD:**

prof.dr. A.D. Nelson (Chair)  
Dr. T. Kauranna (External Examiner, Lappeenranta University of  
Technology Finland)

#### DISCLAIMER

This document describes work undertaken as part of a programme of study at the Faculty of Geo-Information Science and Earth Observation of the University of Twente. All views and opinions expressed therein remain the sole responsibility of the author, and do not necessarily represent those of the Faculty

# ABSTRACT

Tropical forest play a crucial role to the storage of a large amount of carbon, typically the aboveground biomass of trees which is affected by deforestation and degradation. UNFCCC intended to reduce carbon dioxide(CO<sub>2</sub>) emission from land use change and deforestation through (REDD+) program and its MRV Mechanism.

There is a need in tropical countries for low cost, accurate and timely information to determine tree parameters like height and diameter. Direct measurement of tree height with measuring tape is the most accurate, but it is not a viable option for forest monitoring and evaluation. LiDAR is one of the remote sensing technology used to estimate tree height with the best result in terms of accuracy. However, the cost of LiDAR can pose financial constraints, especially when the study area needs temporal data to monitor vegetation change. UAV photogrammetry 3D image photogrammetry using UAV images is a potential cost-effective alternative method. The quality of a UAV-DTM directly influences the estimation of tree height and AGB and carbon stock. The quality of the UAV-DTM in its turn is influenced by number and configuration of the Ground Control Points. Therefore, this thesis present accuracy assessment of UAV DTM with different number and layout of GCPs and its effect on CHM.

The accuracy of UAV DTM with 4,6,8 and ten ground control point, when compared to checkpoints which measured by DGPS, achieved RMSE of  $\pm 0.9$  m and R<sup>2</sup> of 0.98 for all DTMs While R<sup>2</sup> of 0.9 and RMSE of  $\pm 1.5$  m ALS. On the other hand, The accuracy of UAV DTM with 4,6,8 and ten ground control point, when compared to ALS DTM, achieved RMSE of  $\pm 3.6$  m,  $\pm 3.53$  m,  $\pm 3.51$ m, and  $\pm 3.50$  m and R<sup>2</sup> of 0.66,0.68,0.67 and 0.67 respectively.

UAV DTM 8 was selected based on the accuracy assessment result and then tree height derived from UAV CHM for the entire area. The accuracy assessment of UAV tree height in comparison to ALS tree height revealed that RMSE of  $\pm 2.18$  m and R<sup>2</sup> of 0.6. Additionally, the comparison was made between UAV tree height and ALS tree height in relatively Closer altitude of DTM height. The accuracy assessment revealed that R<sup>2</sup> of 0.88 and RMSE of  $\pm 2$  m.

Furthermore, the AGB was computed using an allometric equation which utilized Diameter at Breast height (DBH), tree height and wood density. In order to assess the effect of tree height difference between UAV and ALS on AGB the tree height adjusted based on the accuracy result of UAV tree height. Then AGB and carbon stock computed using the adjusted tree height. The result revealed that mean biomass of 0.04Mg,0.05Mg,0.06Mg and 0.06 for RMSE -2,-1,0,1 and 2 respectively.

**Keywords:** Allometric equation Tree height, DBH, UAV, CHM, DSM, DTM, LiDAR

# ACKNOWLEDGEMENTS

First and foremost, praises and thanks to the God, the Almighty, for His showers of blessings throughout my study here in the Netherlands.

I express my sincere gratitude to Faculty of Geo-information and Earth Observation Science (ITC), University of Twente and Netherland Fellowship Program (NFP) who granted me a scholarship to pursue MSc. degree in Geo-information and Earth Observation Science for Natural Resource Management.

I would like to express my deepest appreciation to my supervisors, Dr. Yousif Ali Hussin, my first supervisor and Drs E. Henk Kloosterman, second supervisor, who has given me constructive and indispensable comments in all phases of the research.

My sincere thanks go to prof.dr. A.D. Nelson for His constructive and genuine comments during the first term and mid-term of proposal defense. I would like to extend my thankful to Drs. Raymond Nijmeijer, NRM, Course Director for tireless continuous of feedback.

I'm indebted to f Universiti Teknologi MARA (UITM) for collaboration in providing Airborne Lidar data and support for fieldwork. I'm very thankful to my Advisor Dr. Zulkiflee Abd Latif Associate Professor at Universiti Teknologi Mara (UITM), for facilitating of the entrance to Malaysia and guidance in fieldwork. I would like to thank Mrs. Syaza Rozali, Ph.D. Candidates at Universiti Teknologi MARA (UITM) for her immeasurable assistance in intensive fieldwork.

Last but not least, my eternal thanks goes to my parents; my father Begashaw Berhanu and my Mother Tesfanesh mahtebu who always helping and encouraging me. You have been patient all the time in my study. My brother yakob and my sisters serkalem, meseret and tselatekidan; I'm always grateful for your encouragement to move forward.

# Contents

LIST OF FIGURES.....	v
LIST OF TABLE.....	vi
LIST OF EQUATION.....	vii
LIST OF ACRONYMS.....	ix
1. INTRODUCTION.....	1
1.1. Background.....	1
1.2. Concept and definitions.....	3
1.2.1. Structure from Motion (SfM) photogrammetry.....	3
1.2.2. Airborne LiDAR.....	4
1.2.3. DTM, DSM and CHM.....	4
1.3. Research problem.....	5
1.4. Objectives.....	6
1.4.1. General objectives.....	6
1.4.2. Specific objectives.....	6
1.5. Research question.....	7
1.6. Hypothesis.....	7
2. MATERIAL AND METHOD.....	8
2.1. Study area.....	8
2.2. Data.....	9
2.3. Flowchart of the method.....	10
2.4. Data collection.....	11
2.4.1. Sampling design.....	12
2.4.2. Biometric data collection.....	12
2.4.3. UAV mission planning.....	13
2.4.4. Ground control point.....	15
2.4.5. UAV image acquisition.....	16
2.4.6. Controlled experiment.....	17
2.5. Data processing.....	17
2.5.1. UAV image processing.....	17
2.5.2. UAV orthophoto segmentation.....	19
2.5.3. Airborne LiDAR data processing.....	20
2.5.4. Extraction of tree height.....	20

2.5.5.	Above-ground Biomass and Carbon Estimation .....	20
2.5.6.	Data analysis .....	21
3.	RESULT .....	24
3.1.	DSM, DTM and Orthophoto Generation from UAV images.....	24
3.2.	Comparison of ALS and UAV photogrammetric image matching DTM .....	25
3.2.1.	Comparison of ALS and photogrammetric image matching DTM'S using Checkpoint recorded by DGPS .....	25
3.2.2.	Comparison of single grid and double grid UAV DTM .....	27
3.2.3.	Comparison of photogrammetric image matching DTM'S and ALS DTM using their height 29	
3.3.	CHM Generation from ALS and UAV photogrammetry and segmentation accuracy assessments .....	31
3.4.	Comparison between the tree heights extracted from UAV-CHM and ALS-CHM .....	32
3.4.1.	Comparison of tree heights extracted from UAV-CHM, and ALS-CHM in areas where the DTMs are nearly the same. ....	34
3.5.	Biometric data.....	36
3.5.1.	Controlled Field experiment .....	37
3.6.	Biomass and carbon estimation.....	37
3.7.	Comparison of UAV-AGB and ALS-AGB.....	38
4.	DISCUSSION.....	41
4.1.	Accuracy of UAV DTM with different number of Ground control point.....	41
4.2.	Source of Tree height variation by UAV photogrammetry .....	42
4.3.	UAV Tree height Estimation.....	42
4.4.	Estimation of above ground biomass and carbonstock.....	43
4.5.	Effect of differences of UAV and ALS tree height on biomass.....	43
4.6.	Limitation .....	44
5.	CONCLUSION AND RECOMMENDATION .....	45
5.1.	Conclusion.....	45
5.2.	Recommendation.....	45



## LIST OF FIGURES

---

Figure 1-1 Structure-from-Motion (SfM). Instead of a single stereo pair, the SfM technique requires multiple, overlapping photographs as input to feature extraction and 3-D reconstruction algorithms. Source : (Westoby et al., 2012).....	3
Figure 1-2 Airborne LiDAR system; points on surface represent at which laser is reflected back. ....	4
Figure 1-3 Difference between DSM and DTM.....	5
Figure 2-1 study area. ....	8
Figure 2-2 Flow chart of the study. ....	11
Figure 2-3 study area shows the part of UAV flight blocks and sample plots. ....	12
Figure 2-4 Study area which consists of young regenerated forest. ....	13
Figure 2-5 Phantom-4 DJI UAV/Drone. ....	14
Figure 2-6 PIX 4D apps. ....	14
Figure 2-7 Distribution of control and checkpoint.....	16
Figure 2-8 Trees which information collected during fieldwork in undulating terrain. ....	17
Figure 2-9 500 Random points for comparison of ALS and UAV DTM.....	21
Figure 2-10 Open space and closed space random point for comparison of UAV and ALS DTM.....	22
Figure 3-1 UAV DSM and DTM.....	24
Figure 3-2 Small part of the ortho-mosaic image generated from the UAV images. ....	25
Figure 3-3 Relationship between UAV DTM'S with different GCPs and checkpoint height. ....	26
Figure 3-4 Relationship between ALS DTM and Checkpoint height. ....	27
Figure 3-5 Comparison of Single and double grid UAV DTM height based on 500 random points.....	28
Figure 3-6 Relationship between single and double grid UAV DTM.....	29
Figure 3-7 Comparison of UAV from ALS DTM height based on 500 random points.....	30
Figure 3-8 UAV Photogrammetry CHM.....	31
Figure 3-9 Sample showing comparison of manually and eCognition delineated tree crown.....	32
Figure 3-10 The scatter plot of ALS-CHM and UAV-CHM extracted tree height. ....	33
Figure 3-11 The scatter plot of ALS-CHM and UAV-CHM extracted tree height in areas where the DTMs are nearly the same. ....	35
Figure 3-12 Effect of differences of field measured tree height on AGB estimation. ....	40

## LIST OF TABLE

---

Table 2-1 Field instruments to be used for the study.....	9
Table 2-2 Software's to be used for the study.....	10
Table 2-3 Settings of the Phantom4 drone for image acquisition.....	15
Table 3-1 Summary of UAV-image processing report using Agisoft Photoscan Professional.....	24
Table 3-2 Accuracy assessment of UAV DTM'S with different GCPs using Check point collected by DGPS. .....	26
Table 3-3 Accuracy assessment of ALS DTM using checkpoint collected by DGPS.....	27
Table 3-4 The t-test assuming equal variance for UAV single and double grid extracted DTM height.....	28
Table 3-5 Summary for comparison of ALS-DTM and UAV-DTMs altitude.....	29
Table 3-6 The t-test assuming equal variance for UAV-DTMS and ALS-DTM in open space.....	30
Table 3-7 Summary for comparison of ALS and UAV DTMs in closed canopy altitude.....	31
Table 3-8 Summary for comparison of ALS and UAV tree heights.....	33
Table 3-9 F-test of two samples for variance.....	34
Table 3-10 The t-test assuming equal variance for ALS and UAV extracted tree height.....	34
Table 3-11 Descriptive statistics of the ALS and UAV measured tree height in the area where DTMs have slightly difference.....	35
Table 3-12 Summary for comparison of ALS and UAV tree heights in areas where the DTMs are nearly the same.....	36
Table 3-13 The t-test assuming equal variance for ALS and UAV extracted tree height in areas where the DTMs are nearly the same.....	36
Table 3-14 Descriptive statistics of DBH height.....	37
Table 3-15 Descriptive statistics for ALS and UAV biomass.....	37
Table 3-16 Summary of relationship and accuracy of UAV computed Biomass.....	38
Table 3-17 Descriptive statistics for ALS and UAV carbon stock.....	38
Table 3-18 Summary of relationship and accuracy of UAV computed carbon stock.....	38
Table 3-19 The t-test assuming equal variance for UAV and ALS computed AGB.....	39
Table 3-20 Effect of differences of measured field tree height on biomass estimation.....	39
Table 4-1 The RMSE error variables of the DTMs interpolated by the four different methods for the two test sites.....	42

## LIST OF EQUATION

---

Equation 2-1: Over segmentation equation model .....	19
Equation 2-2: Under segmentation equation model.....	19
Equation 2-3: Measure of goodness .....	19
Equation 2-4: Allometric equation for above ground biomass .....	20
Equation 2-5 Carbonstock.....	21
Equation 2-6: Equation for RMSE and %RMSE calculation.....	23

## LIST OF APPENDICES

Appendix 1 Data collection sheet. ....	51
Appendix 2 Configuration of GCPs for UAV DTM 4,6,8 and 10.....	52
Appendix 3 t-test to compare height for ALS and UAV DTM's using 500 points.....	53
Appendix 4 t-test to compare height for ALS and UAV DTMs in closed space .....	53
Appendix 5 F-test to compare tree height for ALS and UAV tree heights in closer altitude. ....	54
Appendix 6 matched trees for comparison of UAV and ALS CHM. ....	54
Appendix 7 Comparison of UAV ALS CHM in controlled experiment.....	59
Appendix 8 Relationship between ALS and UAV biomass. ....	59
Appendix 9 Relationship between ALS and UAV carbon stock.....	60
Appendix 10 F-test to compare ALS and UAV AGB.....	60

## LIST OF ACRONYMS

---

AGB	Above Ground Biomass
ALS	Airborne Laser scanning
CF	Carbon Fraction
CP	Checkpoint
CHM	Canopy Height Model
DBH	Diameter at Breast Height
DEM	Digital Elevation Model
DGPS	Differential Global Position System
DSM	Digital Surface Model
DTM	Digital Terrain Model
GCP	Ground Control Points
GPS	Global Position System
GSD	Ground Sample Distance
IMU	Inertia Measurement Unit
IPCC	Intergovernmental Panel on Climate Change
LIDAR	Light Detection And Ranging
MRV	Measurement Report and Verification
NOAA	National Oceanic and Atmospheric Administration
OBIA	Object Based Image Analysis
REDD	Reduce Emission from Deforestation and forest Degradation
RMSE	Root Mean Square Error
SfM	Structure from Motion
UAV	Unmanned Aerial Vehicle
UAS	Unmanned Aerial System
UITM	Universiti Teknologi MARA
UNFCCC	United Nations Framework Convention on Climate Change
WWF	World Wide Fund for Nature



# 1. INTRODUCTION

## 1.1. Background

Forest play a crucial role in in the global carbon cycle by functioning as a sink and a source of carbon (Pan et al., 2011). This function of forest plays a role in carbon dioxide (CO<sub>2</sub>) emission balance. Conversely, forest degradation and deforestation are being major driving agents to the increment of atmospheric carbon dioxide (CO<sub>2</sub>) (Mohren et al., 2012). Tropical forest contributes to the storage of a large amount of carbon, typically the aboveground biomass (AGB) of trees which is affected by deforestation and degradation (Mohren et al., 2012).

Even though the role of forest in carbon sequestration is well known, the CO<sub>2</sub> increment in the atmosphere is one of the main concern since it is a crucial factor for climate change (Crowley, 2000). The anthropogenic factor is driving the increment of CO<sub>2</sub> concentration at an alarming rate. National Oceanic and Atmospheric Administrative (NOAA) show that continuous increment of atmospheric CO<sub>2</sub> currently reached 402.5 ppm which has been 385.05 ppm 10 years back (NOAA, 2017). Anthropogenic greenhouse gas (GHG) emission coupled with lack of information on forest carbon sequestration aggravates the problem (Boudreau et al., 2008).

United Nation Framework on Climate Change (UNFCCC) intended to reduce carbon dioxide(CO<sub>2</sub>) emission from land use change and deforestation through an agreement between different countries. These countries have to report annually on the emission and sequestration from land use change such as deforestation, afforestation, and reforestation (UNFCCC, 1997). To reduce emission from deforestation and forest degradation (REDD+) program was developed to protect forest and ensure accurate Measurement, Reporting and Verification (MRV) of carbon stock of countries. MRV is a mechanism which was established under REDD+ program to enable objective evaluation of the implementation status of REDD-plus policies and emissions and removals for the credit mechanism.

Malaysia is one of the countries that ratified in UNFCC Convention. The country is blessed with diverse rainforests, characterized as unlogged and secondary forest (WWF, 2017).The Ministries of Natural Resources and Environment has the obligation to implement this international convention on monitoring of forest for carbon sink. REDD+ was developed for implementation on the national and sub-national level of forestry which plan to implement MRV techniques. Thus, exploring a cost-effective method for providing accurate and timely information to determine forest parameter has been given central emphasis. Various methods are developed, destructive as well as non-destructive, to accurately estimate forest biomass and carbon stock. The latter using biometric parameters, such as DBH and tree height in combination with an allometric equation. to estimate aboveground biomass/ carbon stock (Brown, 2002a).

Destructive sampling methods provide an accurate biomass estimation. It involves in cutting and weighing trees, which is a labor-intensive, time-consuming, hence expensive and environmentally unfavorable method. A non-destructive method using an allometric equation is widely recognized method for carbon stock estimation. The allometric equation derived from regression model which needs input parameter of field measured tree height and diameter at breast height (DBH) (Brown, 2002b; Chave et al., 2014). Even though field based estimation of forest carbon stock is commonly used, it lacks field inventory data in remote areas

which is a constraint for reliable biomass estimation. Ground inventory demands tedious efforts over large areas and is not well suited for monitoring carbon stock change over time.

Unreliable estimate of AGB occurs due to tree parameters measurement errors. Tree height measurement using a traditional field-based instrument, such as hypsometer and handheld laser, are sensitive to measuring errors due to forest stand structure. Especially, traditional field-based tree height measurement in the tropical rainforest is associated with inaccurate tree height measurement due to multilayer structure (Bazew, 2017; Reuben, 2017). Bazew (2017) highlighted that handheld laser instrument in closed canopy forest result inaccurate tree height measurement due to occlusion effect.

The need for monitoring change in forest carbon stock and use of earth observation data has been grown continuously to acquire forest inventory data over a large area at a regular time interval. This multi-temporal remote sensing approach could improve spatial forest inventory and reduce efforts in field inventory.

Light Detection and Ranging (LiDAR), which uses an actively emitted laser beam as its base for measuring the physical aspect of objects, is a more recent remote sensing technology. LiDAR can provide data on the vertical structure of a forest through scanning with a laser pulse (Jung et al., 2011; Pirotti, 2011). Different research showed that LiDAR is very suitable for generating a canopy height model (CHM) and trees height extraction, with high accuracy (Andersen et al., 2006; Ferraz et al., 2016; Hyypä et al., 2012). Unfortunately, the acquisition of LiDAR data is often too expensive for regular forest monitoring (Pirotti, 2011).

Structure from motion (SfM), or 3D Photogrammetric image matching, using a digital camera mounted on small, low-cost Unmanned aerial vehicle (UAV) system is a cost-effective alternative remote sensing technology. SfM is built on the principle of the traditional stereoscopic view technique. The 3D structure of an object can be perceived from a series of overlapping images, using parallax. UAV Photogrammetry provides a computation of metrics measurement of aerial photographs of an object without having any physical contact (Ordóñez et al., 2010).

One of the benefits of UAV over ALS technology is that they can be autonomously programmed to complete repetitive missions with high precision (Unmanned Aerial Vehicle Systems Association Advantages of UAVs, 2017). In addition to that, it has the flexibility to bring the device to the field at very short notice and, UAV has a high repeatability and flexibility in data acquisition process (Fritz et al., 2013). UAV has been used to measure forest parameter with good results in terms of accuracy (Kachamba et al., 2016; Lim et al., 2015).

However, a vital component of estimating canopy height and forest parameter from any 3D remote sensing product is the ability to accurately characterize ground topography in the form of a Digital Terrain Model (DTM) (Drake et al., 2002). Therefore, assessing the DTM accuracy of UAV point cloud to determine forest parameter is essential.

LiDAR provides accurate 3-D point clouds suitable for Digital terrain model (DTM) and Digital surface model (DSM) construction, which are important for accurate measurement of tree height (Popescu et al., 2002). The accuracy of a DTM derived from UAV point clouds depends on accurate UAV image bundle block adjustment, which depends on configuration and distribution of Ground Control Points (GCP) (Nex and Remondino, 2013). Therefore the GCPs have a direct influence on UAV-DTM and subsequent tree height estimation.

An accurate DTM can be created in a forest where a clear view of forest ground is available (Ota et al., 2017; Wallace et al., 2016). However, the UAV photogrammetric technique underperformed in capturing the terrain surface under increasingly denser canopy cover in the complex tropical rain forest (Ota et al., 2015). Limited



literature is available in assessing the accuracy of UAV DTM in the tropical rainforest. This study was aiming to assess the accuracy of UAV DTM with different number of ground control point and layout.

## 1.2. Concept and definitions

### 1.2.1. Structure from Motion (SfM) photogrammetry

Structure from Motion finds its origin in the machine vision community, particularly for finding tracking points across a sequence of images, from different positions and angles (Spetsakis & Aloimonos, 1991). SfM is based on innovations and mathematical models developed many generations ago, particularly in photogrammetry (Micheletti et al., 2015). Photogrammetry provides a computation of metrics measurement of aerial photographs about an object without having any physical contact (Ordóñez et al., 2010).

SfM has built on the principle of a traditional stereoscopic technique, namely that 3D structure can be resolved from a series of overlapping images (figure1-1). The advancement in computer vision algorithms, such as Scale-invariant Feature system (SIFT) and Parallel Bundle Adjustment of graphics processing units, allow the SfM technique to generate 3D point clouds from photographs acquired from small UAVs (Zarco-Tejada et al., 2014).

UAV photogrammetry is a helpful tool in topographic applications, surveillance, live video monitoring, forest monitoring etc. Their cost-effectiveness and availability has motivated researcher to explore the use of UAV in different fields, such as crop monitoring and precision farming (Zarco-Tejada et al., 2014), biomass estimation (Kachamba et al., 2016), etc. Recent studies show that attributes like tree height and canopy dimension of a tropical lowland rainforest can be derived successfully from 3D Point clouds derived from overlapping UAV images (Lim et al., 2015; Reuben, 2017). Forest biomass estimation from UAV imagery depends on how accurate forest parameter can be estimated from overlapping images.

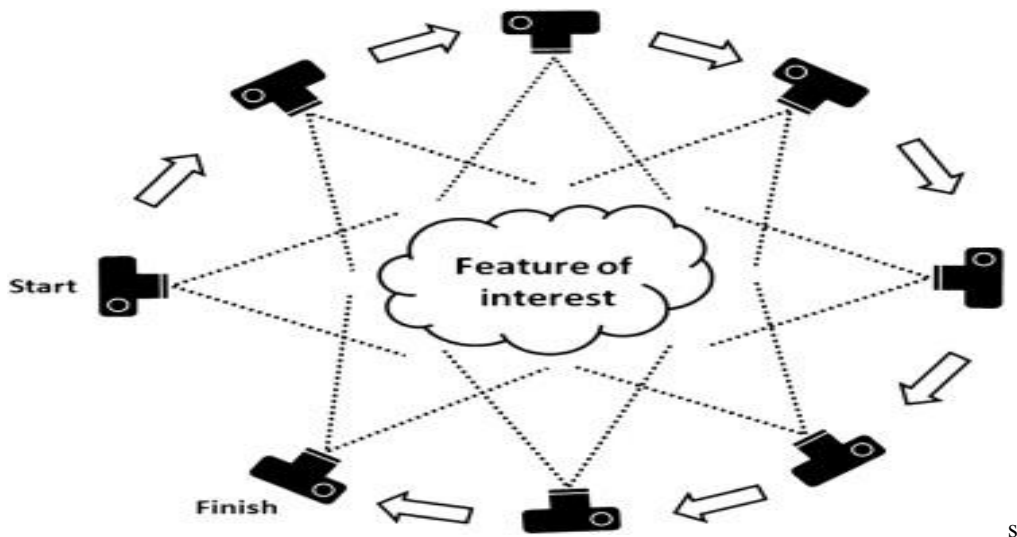


Figure 1-1 Structure-from-Motion (SfM). Instead of a single stereo pair, the SfM technique requires multiple, overlapping photographs as input to feature extraction and 3-D reconstruction algorithms. Source : (Westoby et al., 2012)

### 1.2.2. Airborne LiDAR

Airborne LiDAR is an active remote sensing technology and stands for Light Detection and Ranging. It is also called Airborne laser scanning (ALS). LiDAR uses near-infrared radiation ranging from 90 to 1064 nm as a source of illumination and provides 3D geometry of objects using small beam width, multiple pulses, and waveform digitization (Wehr & Lohr, 1999). Airborne LiDAR consists 3 components: (i) Laser device for accurate distance measurement, (ii) higher precision GPS which record position of the aircraft and (iii) Inertial Measurement Unit (IMU) to record orientation (figure 1-2). The laser unit determines the distance between aircraft and the targeted object using the travel time of emitted and reflected pulse. LiDAR technology provides accurate Digital Terrain Model (DTM), which is helpful to estimate the vertical structure of forest tree height extraction (Andersen et al, 2006; Leitold et al, 2015).

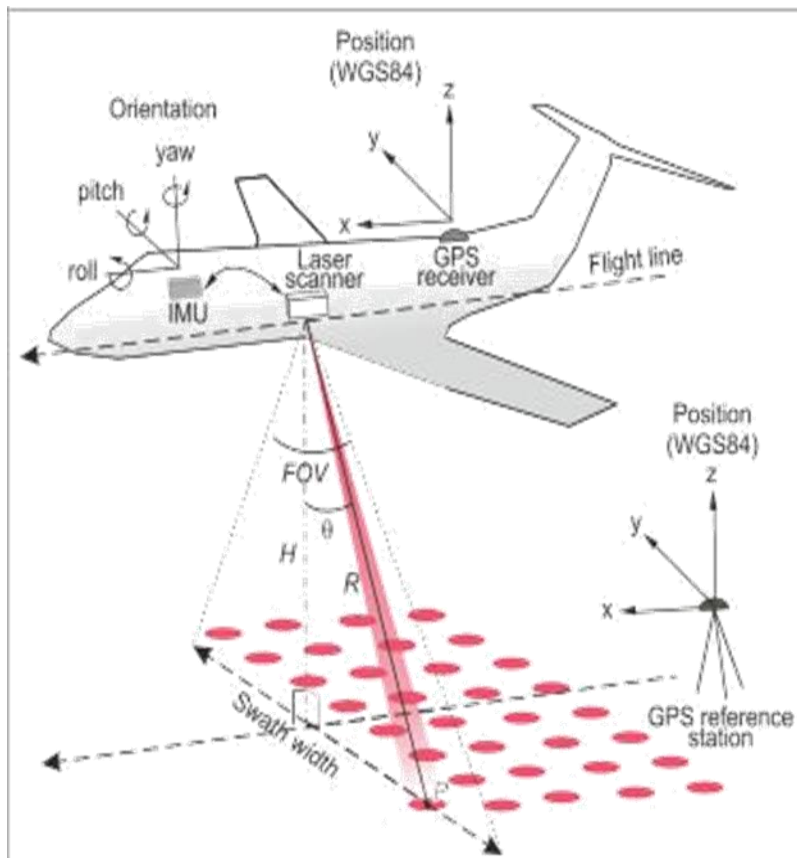


Figure 1-2 Airborne LiDAR system; points on surface represent at which laser is reflected back.

Source: Gally (2013)

### 1.2.3. DTM, DSM and CHM

Digital surface model (DSM) depicts the height values of the surface including the objects (for instance a forest) on it, while Digital Terrain Model (DTM) is a topographic model of the underlying terrain, without the objects (for instance a forest) on it (figure 1-3). A Canopy Height Model (CHM) is a difference between the (DSM), and the DTM.

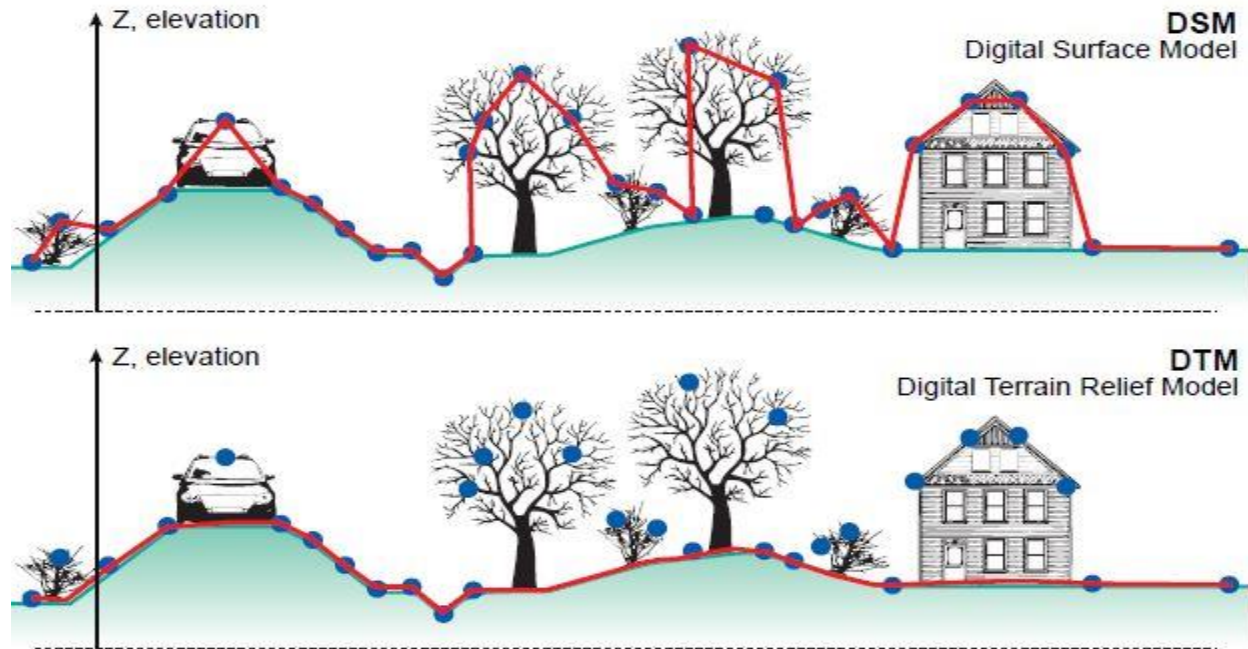


Figure 1-3 Difference between DSM and DTM.

Source: <http://www.charim.net/datamanagement/32>

### 1.3. Research problem

Reducing greenhouse emission from deforestation has been long identified as having great potential for global climate change mitigation (Böttcher et al., 2009). This case is particular in developing countries where the major source of GHG emission is coming from land use change and forest loss (Gibbs et al., 2007). REDD+ initiated a program to counteract climate change due to GHG emission in forest-rich developing countries (UNFCCC, 2010). Through REDD+ countries gain economic incentives by demonstrating quantifiable emission reduction by protecting their forest. However, the success of REDD+ depends on a consistent methodology for monitoring reporting and verification (MRV) so the incentives paid can be evidence based for carbon emission reduction (Gibbs et al., 2007). This leads to anticipated demand in tropical countries for low cost, accurate and timely information to determine forest parameters.

Measurement, reporting, and verification ( MRV ) of forest carbon stock is performed for REDD+ and the UNFCCC has suggested the use of remote sensing techniques for this purpose (REDD+, 2012). It includes very high resolution (VHR) optical sensors, Synthetic Aperture Radar (SAR) and Light Detection And Ranging (LiDAR) for Above Ground Biomass (AGB) and carbon stock monitoring.

In order to build and validate remote sensing based forest AGB models, field based AGB measurements are a requirement. As was discussed in the introduction, allometric equations provide a non-destructive and efficient way to estimate AGB using tree parameters like height and DBH. Tree height improves biomass estimation as compared to DBH only allometric model (Chave et al., 2005; Chave et al., 2014). Direct measurement of tree height with measuring tape is the most accurate, but it is not a viable option for forest monitoring and evaluation. Handheld height measurement equipment like a rangefinder are an alternative, but accurate tree

height measurements in the complex tropical rain forest is problematic (Bazezew, 2017). Tree height can be estimated using remote sensing data.

LiDAR is one of the remote sensing technology used to estimate the vertical structure of a forest, including tree height, and produces the best results in terms of accuracy (Andersen et al., 2006; Zolkos et., 2013). However, the cost of LiDAR can pose financial constraints, especially when the study area needs temporal data to monitor vegetation change.

3D image photogrammetry using UAV images is a potential cost-effective alternative method. Structure from motion (SfM) allows the extraction of a 3-D point cloud from a two-dimensional image sequence. The SfM method extracts the 3-D structure of a scene from overlapping images using bundle adjustment procedure (Micheletti et al., 2015). The resulting 3-D point cloud can be used to construct a DSM, a DTM and a CHM, and also for the extraction of forest parameter, like stand density and tree height (Næsset et al., 2004).

In order to obtain reliable tree heights from remote sensing data, an accurate DSM, and DTM are pivotal, since they determine the quality of the CHM and subsequent tree heights (Maltamo et al., 2004; Næsset et al., 2004; Paper & Stere, 2008). In other words, the quality of a UAV-DTM directly influences the estimation of tree height and any AGB estimate based on those tree heights

The quality of the UAV-DTM in its turn is influenced by number and configuration of the Ground Control Points (GCP) (Nex & Remondino, 2013; Niyonsenga, 2016; Tahar, 2013). It is due to the fact that GCPs have an impact on bundle block adjustment, which is the first step in the process of 3-D point cloud extraction and subsequent DTM calculation. In short, the number and layout of GCPs influence quality of UAV-DTM, which in its turn determines the quality of the UAV-CHM.

Limited literature is available concerning UAV-DTM accuracy assessment and its effect on the canopy height model (CHM) and subsequent AGB estimates in tropical lowland rainforest.

## **1.4. Objectives**

### **1.4.1. General objectives**

The main objective of this research is to assess the accuracy of a Digital Terrain Model derived from a UAV based 3-D point cloud, in relation to number and distribution of the Ground Control Points and its effect on the Canopy Height Model and Above Ground Biomass estimations, in a part of a tropical lowland rainforest, Berklah , Malaysia.

### **1.4.2. Specific objectives**

1. To assess the accuracy of a DTM derived from UAV 3D point cloud with different number and layout of GCPs by comparing it to Airborne LiDAR DTM.
2. To extract a CHM and tree height from UAV 3D point cloud and compare it to a LiDAR CHM and tree height.
3. To assess the effect of the tree height differences on the AGB and carbon stock calculation.

### 1.5. Research question

1. What is the accuracy of DTM derived from UAV in relation to number and layout of GCPs in comparison to the DTM derived from Airborne LiDAR?
2. What is the accuracy of tree heights derived from the UAV based CHM in comparison to tree heights derived from the LiDAR based CHM?
3. How are AGB and carbon stocks estimates affected by tree height difference between UAV and LiDAR based data?

### 1.6. Hypothesis

1. **H<sub>0</sub>**: There is no significant difference in the UAV based DTM, using a different number and layout of GCPs and the Airborne LiDAR DTM  
**H<sub>1</sub>**: There is significant difference in DTM generated using different number of GCP and Airborne LiDAR DTM
2. **H<sub>0</sub>**: There is no significant difference in tree heights derived from the UAV-CHM and the tree heights derived from the LiDAR-CHM.  
**H<sub>1</sub>**: There is a significant difference in tree heights derived from the UAV-CHM and the tree heights derived from the LiDAR-CHM
3. **H<sub>0</sub>**: There is no significant difference between AGB using UAV tree height and AGB using ALS tree height-  
**H<sub>1</sub>**: There is a significant difference between AGB using UAV tree height and AGB using ALS tree height

## 2. MATERIAL AND METHOD

### 2.1. Study area

The study was carried out in Berkelah Forest Reserve, which situated in near Kuantan in the state of Pahang. It lies roughly between latitude  $3^{\circ}46'1''\text{N}$  and longitude  $103^{\circ}1'1''\text{E}$  and it is about 234 km to the north-east of Kuala Lumpur (figure 2-1). The forest classifies as tropical lowland rainforest and is characterized by species of *Dipterocarpaceae* family (Omar et al., 2015).

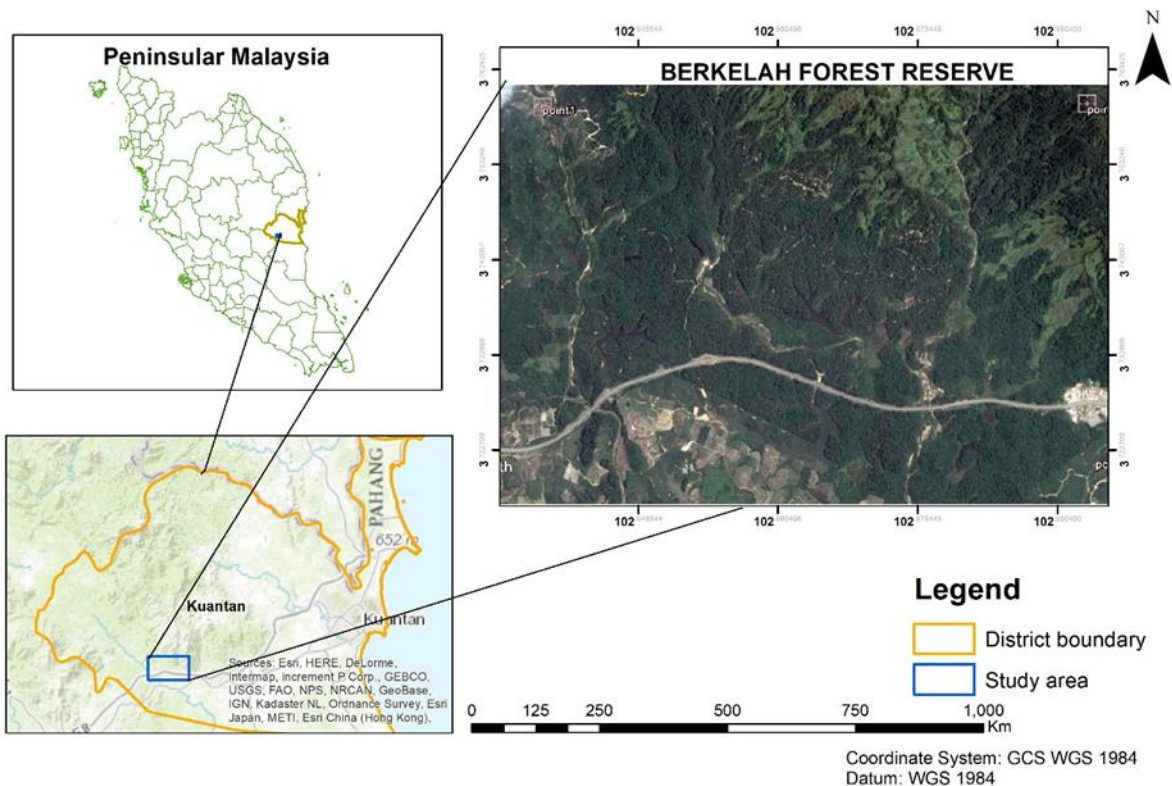


Figure 2-1 study area.

Berkelah forest reserve is situated near the equator and the climate is characterized by high humidity, uniform temperature, and heavy rainfall with average annual precipitation around 2900mm. The climate is classified as a tropical rainforest, with two seasons each year - dry and hot, and very wet. The hot, dry season is due to the blocking of the south-west winds, blowing from the land mass of Sumatra towards Peninsular Malaysia's west coast by the Titiwangsa mountains (Malaysian Meteorological Department, 2017). The mean monthly temperature ranges from  $24.2^{\circ}\text{C}$  to  $29.9^{\circ}\text{C}$  while the average monthly rainfall ranges from 90 mm to 300 mm, with an air humidity of 70% to 98%. The landscape of the study area is undulating terrain with several different topographical characteristics such as hillsides, ridge, and valley. The terrain is moderately steep slope and elevation roughly ranges from 43-110m.

## 2.2. Data

Airborne LiDAR scanner (ALS), UAV images, field-based forest parameters and Ground control point were used for this study. The UAV images and field-based parameter were collected from September 22, 2017 to October 13, 2017. The ALS data provided by Universiti Teknologi MARA (UTM) was acquired on November 12, 2014. GCP were measured using Differential Global Positioning System (DGPS). The UAV image used to acquire 3d point clouds which used to provide DTM, DSM, and CHM. The LiDAR data was used to provide DTM, DSM, and CHM. The GCP was used to georeferencing UAV images and assess the accuracy of DTM of UAV and LiDAR. Next, to that DBH and XY coordinates of tree and centre of the plot were measured in the field.

To collect UAV images, design sample plot and tree parameter measurement various field instruments were used. Details of them with their purpose stated in Table 2-1.

Table 2-1 Field instruments to be used for the study.

S. No.	Instrument	Purpose
1	Chalk	To mark measured trees
2	Diameter Tape	Tree DBH measurement
3	GPS	Navigation, plot and tree location record
5	I pad	To import map for navigation
6	Orthophoto image	Sampling design
7	Measuring tape	Plot layout measurement
8	Stationaries(Pencil, Datasheet, Clipboard, Marker)	Measurement recording
9	Differential GPS	To measure GCP(ground control point)
10	UAV Phantom 4 DJI	To capture image
11	Suunto clinometer	Slope measurement

Various software packages were used to extract, analyze and present ALS, UAV and field data sets. Details of used software's are provided in Table 2.2

Table 2-2 Software's to be used for the study.

S. No.	Software	Purpose
1	ArcGIS 10.5	Data processing, Mapping, Visualization and ALS data processing
2	Agisoft PhotoScan	UAV imagery processing
3	eCognition	Image segmentation
4	ERDAS IMAGINE 2016	For image analysis
5	Microsoft Excel	Data processing and analysis
6	Microsoft power point	Presentation of thesis
7	Microsoft Word	For thesis writing
8	Las tool	To Display LiDAR data
9	Lucid chart	For flowchart drawing
10	R-statistics	Statistical analysis
11	Mendeley	For citation and reference writing

### 2.3. Flowchart of the method

The method used in this study consists of four (4) parts (see figure 2.2):

1. Field data collection  
output: Diameter at Breast Height of the trees inside a field plot
2. UAV image processing  
output: Five (5) DTMs with different number and layout of GCPs, and tree height
3. Processing of the LiDAR data  
output: DTM and tree height
4. AGB biomass estimation and comparison  
output.



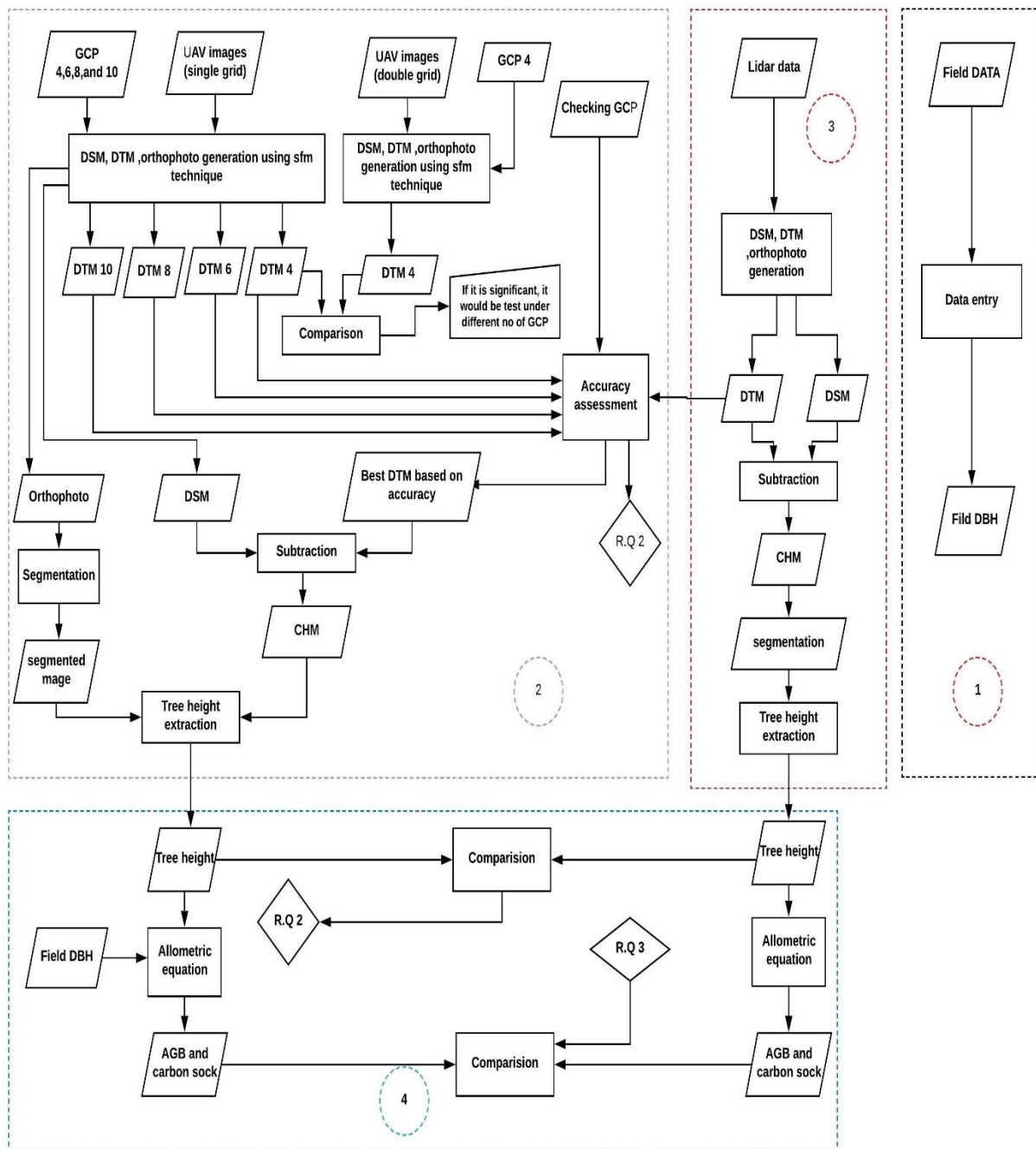


Figure 2-2 Flow chart of the study.

## 2.4. Data collection

This section describes the field data collection and UAV image acquisition, including the layout and DGPS recording of the GCPs.

### 2.4.1. Sampling design

In order to cover the variation in forest conditions and taking terrain conditions, the accessibility of the forest, slope steepness, presence of roads and time constraints into consideration, a purposive sampling approach adopted. The UAV flight areas were selected based on the availability of open space to place ground control points.

Circular plots were used; with a size of 500 m<sup>2</sup> (radius 12.6 m). A circular plot is relatively easy to set and minimizes the number of trees standing on the edge.(Kershawe et al., ; Maniatis & Mollicone, 2010). In sloping areas, a slope correction factor was applied to maintain an area of 500m<sup>2</sup> when vertically projected.

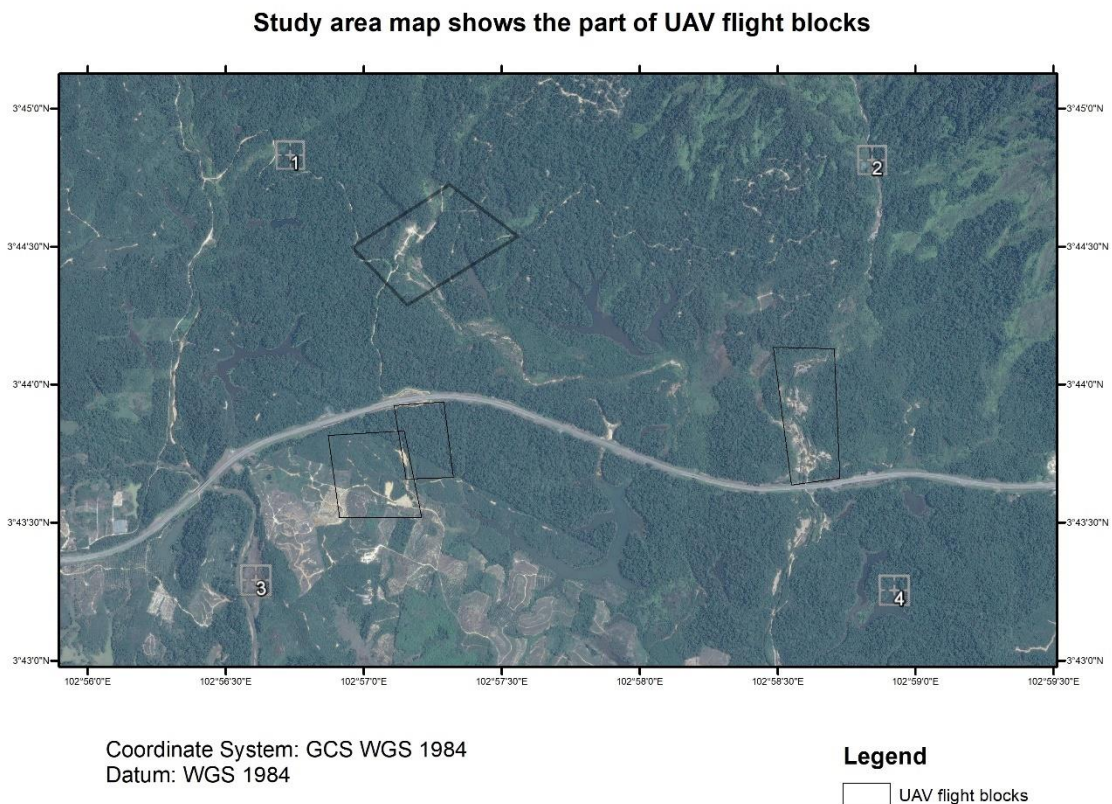


Figure 2-3 study area shows the part of UAV flight blocks and sample plots.

### 2.4.2. Biometric data collection

Fieldwork was done in September and October 2017. Once the centre point of the plot was established, a measuring tape was used to set the plot radius (12.62m) in order to arrive at a sample plot size of 500 m<sup>2</sup>. The XY coordinates of the centre as well as the individual trees was recorded with a handheld GPS. The DBH of the trees inside the plot was measured with a measuring tape. All data were entered in a data sheet that was prepared prior to the field work (see appendix 1). Normally trees with a DBH smaller than 10 cm are excluded since their contribution to the AGB of a forest is negligible (Brown, 2002b). For this study, it was key to have

sufficient open spaces to be able to vary number and position of the GCPs (see also section 2.3.1.3). The only accessible area meeting this requirement was at the South West border of the fieldwork area (see figure 2-3). Unfortunately, a part of this area consists of relatively young regenerating forest (fig 2-4) with very few trees with a DBH larger than 10 cm. Excluding trees with a DBH smaller than 10 cm would lead to a gross underestimation of the biomass. For this reason, it was decided to lower the threshold and include all trees with a DBH of 5cm or more, assuming that this would not affect the outcome of the AGB calculation using the allometric equation.



Figure 2-4 Study area which consists of young regenerated forest.

#### **2.4.3. UAV mission planning**

The UAV dataset used in this study consists of the imagery acquired in four areas in Berklah forest reserve. The flight areas were identified based on the availability of open space for placing ground control points. The UAV images were acquired by using Phantom 4 DJ (figure 2-5).





Figure 2-5 Phantom-4 DJI UAV/Drone.

The mission planning was done in PIX 4D apps (capture and Pix4D Ctrl DJI) (fig xx) using the settings as presented in Table 2-3, taking into consideration that the maximum flying height in Malaysia is 150 m and the flying time per mission should not exceed the capacity of the batteries. The area was recorded twice, with perpendicular flight lines, in order to assess the effect of using a single or double grid on the UAV-DTM. The area for taking off and landing was located in the highest part of the area to be recorded, to ascertain the radio contact with the drone.

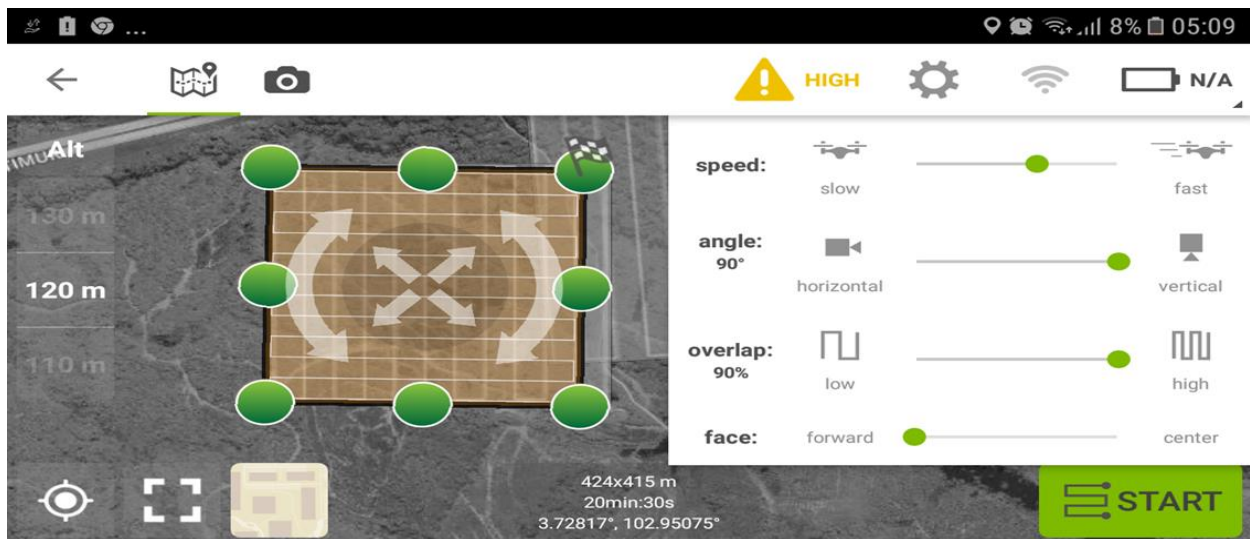


Figure 2-6 PIX 4D apps.

Table 2-3 Settings of the Phantom4 drone for image acquisition.

Parameter	Value
Speed	Moderate
Angle	90 (Nadir)
Overlap	80%
Side Overlap	60%
Altitude Area 1 till 4 and 6	120 m

The highest possible overlap (80% forward overlap and 60-80% side overlap) provides more common points (key points) and allow to compensate for aircraft instability during photo alignment, resulting in a more accurate 3-D point cloud (Colomina & Molina, 2014).

#### 2.4.4. Ground control point

UAV photogrammetric output is normally lower in quality compared to professional manned airborne systems. This has as a consequence that in order to achieve high accuracy products, incorporating Ground Control Points (GCPs) is required (Gerke & Przybilla, 2016).

In this study, the analysis of the effect of number and layout of GCPs was an essential step, because it complies with the objectives of this study. The UAV flight areas were identified in such a way that all areas have had enough open spaces for placing GCPs. The set control point was split in two, the GCP's used in the UAV image processing and the checkpoints which were used for accuracy assessment. In every point, a marker was placed, consisting of a large piece of cardboard with a black and white circle sprayed on it with spray to provide good contrast and ensure visibility in the UAV images flying at 120 m altitude (figure 2-7). They were used for georeferencing and the checkpoints were used to assess the UAV DTM accuracy (figure 2-7). A total of 10 GCPs and 6 checkpoints were placed in one flight block. The GCPs and checkpoint locations were measured with high accuracy using a Differential GPS system.

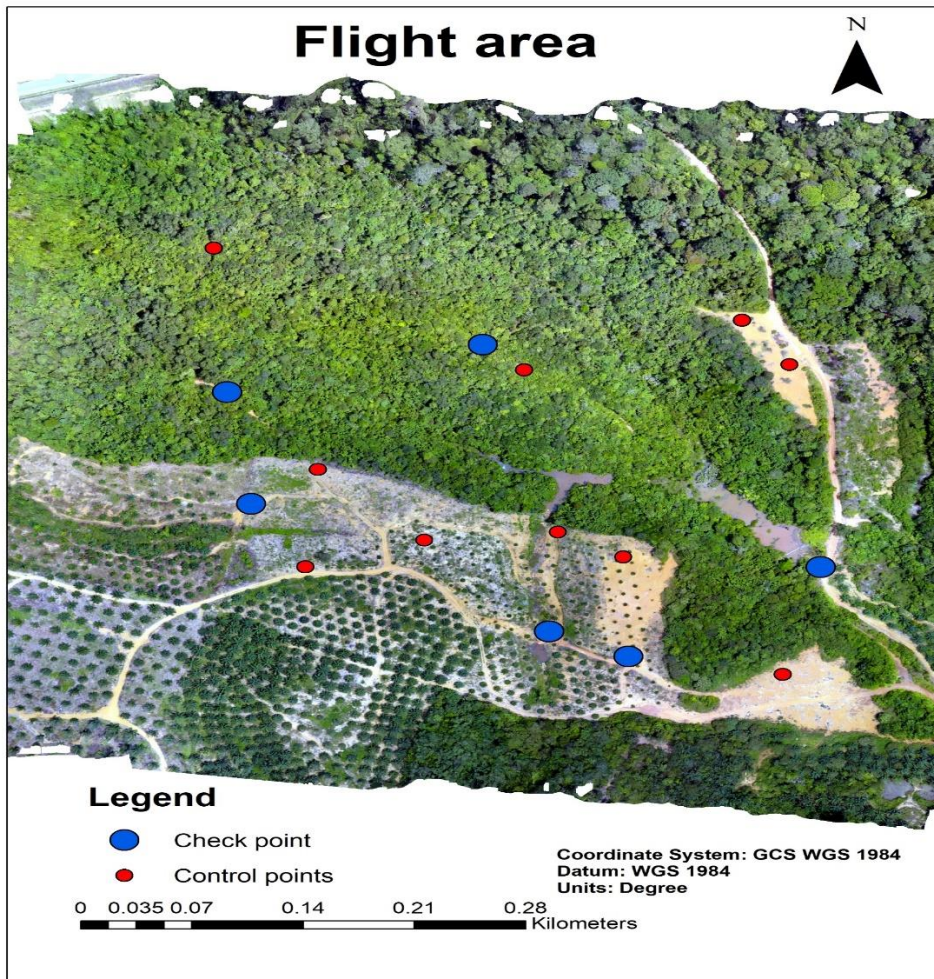


Figure 2-7 Distribution of control and checkpoint.

#### 2.4.5. UAV image acquisition

Before takeoff the settings (see figure 2-6) and battery capacity were checked. All the images were stored on the UAV memory card, transferred onto a laptop and their quality evaluated directly after completion of the mission.



### 2.4.6. Controlled experiment

In order to understand and investigate the effect of canopy closure and undulating terrain on UAV tree height estimation, these controlled field experiment was conducted. For the purpose, these experiment DBH and XY coordinates of selected 10 trees were collected in steep slope and undulating terrain (figure 2-8). This area was located in the second flight block at south west of the study area.

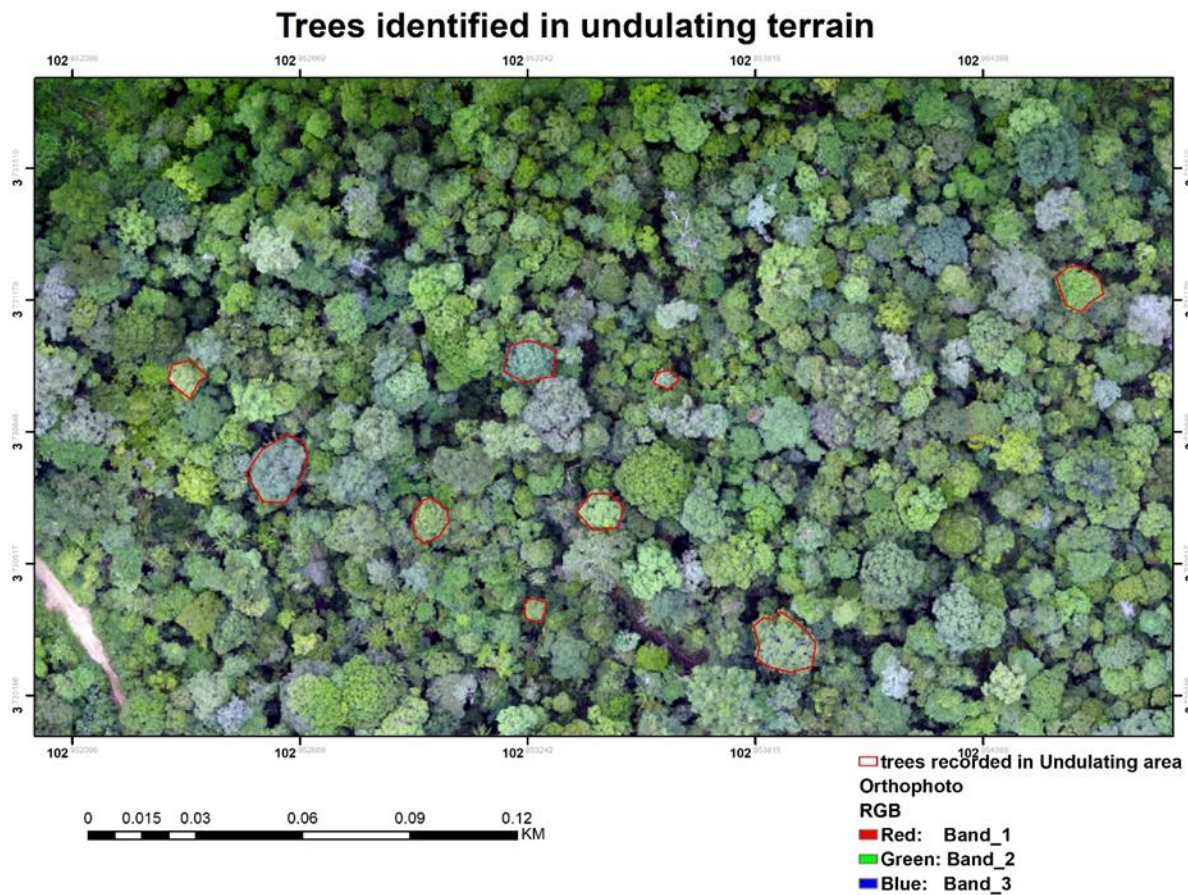


Figure 2-8 Trees which information collected during fieldwork in undulating terrain.

## 2.5. Data processing

### 2.5.1. UAV image processing

The photogrammetric software Agisoft® Photoscan Professional was used to generate a 3-D point cloud, DTM, DSM and orthophoto from the acquired images. Agisoft was also used in a study done by Kachamba et al., (2016) because of its capability to provide dense point cloud in a vegetated area. This software uses both SfM and stereo-matching algorithms for image alignment and multi-view stereo reconstruction. SfM involves a process that automatically finds and matches a large number of common features between photos which are then used to establish both interior and exterior orientation parameters. A subsequent procedure then extracts

a high resolution and colour-coded point cloud to represent the object (Micheletti et al., 2015). Processing of the images with Photoscan consists of the following step (Kachamba et al., 2016; Torres-Sánchez et al., 2015):

- Image orientation and Alignment
- Marker Placement (GCPs’)
- Optimization of camera alignment
- Dense point cloud generation
- Building DSM and DTM and Orthomosaic

### **Image orientation and alignment**

The images were uploaded to the software (Agisoft Photoscan). At this stage, PhotoScan finds the camera position and orientation for each photo, key points and tie points and builds a sparse point cloud mode. In this study, “high accuracy” setting was used since it helps to obtain more accurate camera position estimates, and hence improves photo-alignment and results in a more accurate sparse point cloud.

### **Marker Placement (GCPs’)**

There are two approaches of marker placement in Agisoft photoscan, manual marker placement, and guided marker placement. The manual approach was applied in this study where the ground control points were manually identified and indicated on each photo where the marker was visible. GCP’s were used in each block to improve the image alignment and georeference the generated model. In order to analyze the effect of number and layout of the GCPs on the UAV DTM, the images were processed with 4, 6, 8 and 10 GCPs in different configurations (see Appendix 2)

### **Optimization of camera alignment**

To achieve higher accuracy in calculating camera external and internal parameters and to correct possible distortion the Optimization procedure was executed (Agisoft, 2017). The optimization involved two steps. First, the sparse point clouds were edited manually by removing noticeable outliers and misallocated points and secondly the GCPs were used to run the optimization process. The GCPs locations were measured in the field with high accuracy by a Differential GPS system.

### **Dense point cloud extraction**

After camera optimization, the dense 3-D point was generated, using the “high quality” setting of the software.

### **DSM, DTM, and orthophoto generation**

Agisoft Photoscan software allows for the automatic generation of a Digital Surface Model (DSM) and Digital Terrain Model (DTM). After building the 3-D dense point clouds and 3-D polygonal model the software generated a DSM and Orthomosaic. Prior to the generation of the DTM, the dense point cloud was classified in in two classes, viz. “ground” pixels and “other”. The software uses an algorithm to identify the “ground” pixels and generates a DTM based on these pixels only, resulting in a topographic model of the bare ground or underlying terrain.



## CHM generation

The DTM and DSM were exported to ArcGIS and with the “Raster calculator” tool the DTM was subtracted from the DSM in order to arrive at the CHM. The CHM is the input for tree height extraction (see section 2.5.4)

### 2.5.2. UAV orthophoto segmentation

The orthophoto was segmented by using eCognition software. Segmentation is a technique of spatial clustering in which an image is subdivided into non-overlapping objects or segments (Möller et al., 2007). The process involves image partitioning in more or less homogeneous areas representing an individual tree crown based on an interactive rule set. In this study, multi-resolution image segmentation approach was used. This method follows a bottom-up algorithm, where pixels are merged into real-world large objects until no more adjacent pixels comply the algorithm setting (Definiens, 2009). The rule set was developed for a small subset of the whole image and was later applied to the whole study area. Segmentation was done in order to delineate the crown of individual trees. Individual tree identification was important because it was used for matching ALS and UAV based tree height data, which were used to analyze the effect tree height difference on AGB and carbon stock.

After segmentation an accuracy assessment was conducted to compare the number of trees identified by tree matching, assuming each image segment was a single tree as stated by (Yao et al., 2014). For this step a number of trees crown visible in the orthophoto were manually delineated and compared with the corresponding segment on the eCognition output, using equation 2-1, 2-2 and -2-3.

Equation 2-1: Over segmentation equation model

$$\text{Over segmentation}_{ij} = 1 - \frac{\text{area}(X_i \cap Y_j)}{\text{area}(X_i)} \dots\dots\dots 1$$

Equation 2-2: Under segmentation equation model

$$\text{Under segmentation}_{ij} = 1 - \frac{\text{area}(X_i \cap Y_j)}{\text{area}(Y_j)} \dots\dots\dots 2$$

Where;

xi Reference object manually segment the crown (On screen digitized objects)

yj Corresponding segmented object by eCognition

Equation 2-3: Measure of goodness

$$D = \sqrt{\frac{\text{over segmenation}^2 + \text{under segmenation}^2}{2}} \dots\dots\dots 3$$

Where;

D is closeness of fit or segmentation goodness

The value of under segmentation and over segmentation lies within the range of 0 to 1, where 0 value for both under and over segmentation means perfect segmentation, that is the training object perfectly match with the segments (Clinton et al., 2014). The segmentation goodness or closeness of fit (D) is a measure of error in segmentation (equation 2-3). The D value lies between 0 and 1, where 0 means perfect segmentation.

**2.5.3. Airborne LiDAR data processing**

Airborne LiDAR dataset was given by Universiti Teknologi MARA (UITM). The ALS point cloud density was 5 points/m<sup>2</sup>. Airborne LiDAR dataset was given by Universiti Teknologi MARA (UITM). The ALS point cloud density was 5 points/m<sup>2</sup>. The LiDAR data was processed in Arc Map 10.5.1 to provide DSM and DTM. DTM was generated from the ground returns, while DSM created from the first return (Esri, 2011). The Triangulated Irregular Network (TIN) interpolation method was performed to generate DSM, DTM, and CHM in the ArcGIS program. This process converted LiDAR points into a raster format (Boudreau et al., 2008; Jung et al., 2011).

**2.5.4. Extraction of tree height**

Tree height extraction was done using UAV and ALS CHM, which derived by subtracting DTM from DSM. Then, the segmented orthophoto shapefile, field circular plot, recorded centre plot and individual tree location was later overlaid on the UAV-CHM as well as the ALS-CHM. The UAV-CHM was co-registered with the ALS-CHM to ensure a perfect spatial match. The maximum elevation was used to identify tree height using ArcMap 10.5.1. Identification of the individual trees was done by overlaying the coordinates of the trees as recorded in the field on the segmented image. Due to the error in the GPS measurements, this was not a perfect fit and the final step was to visually compare the pattern of the coordinates as recorded in the field with the pattern of the segmented tree crowns in order to determine which segment belongs to which individual tree in the field. The quality of the DTM is influenced by the density of the points at terrain level and the CHM and subsequent tree height are directly depending on the DTM. In areas with a closed canopy, the differences in ALS-DTM and UAV-DTM are expected to be larger. For this reason, 154 trees, 60 trees from first flight block, 18 trees from second flight block and 76 trees from the third flight, were selected in areas where there was a small difference in altitude between ALS-DTM and UAV-DTM and the tree heights were compared by means of a t-test.

**2.5.5. Above-ground Biomass and Carbon Estimation**

The allometric equation of Chave et.al (2014) was used for AGB estimation. This equation contains a species-specific wood density constant, but in areas, with a diverse species composition the use of species-specific allometric equations is not feasible (Gibbs et al., 2007). Since the study area is a forest contains high diversity in tree species, the AGB was estimated based on the generic wood density for tropical forest developed by Chave et al. (2014) (see equation 2-4).

Equation 2-4: Allometric equation for above ground biomass

$$AGB = 0.0673 * (\rho * D^2 H)^{0.976} \dots \dots \dots 4$$

Where,

AGB-Above-ground biomass (kg); D-Diameter at breast height (DBH) (cm); H-height (m); and  $\rho$ -wood density (g/cm<sup>3</sup>).

Above-ground biomass will be converted to carbon stock. Carbon amount is approximately 47% of the dry biomass of the tree. For this study, the conversion factor by IPCC, (2006) was used.

Equation 2-5 Carbonstock

$$C = B \times CF \dots\dots\dots 5$$

Where C is Carbon stock (Mg), B representing the biomass and CF is the fraction of the carbon in the biomass (0.47)

**2.5.6. Data analysis**

The comparison of ALS DTM and UAV photogrammetric image matching DTMs which processed with 4, 6, 8 and 10 GCPs in different configuration were compared using random points. Since large dataset reduces uncertainties, arbitrary 500 random points(see figure 2-9 ) used for comparison in the area of interest. Arc-Map 10.5.1 was used to Setout randomly distributed points and extract DTM'S value. These 500 random points also used for comparison of single and Double grid UAV DTMS.

Furthermore, UAV DTMS and ALS DTM comparison compared in open and closed space by classifying 500 random points into open and closed space(closed canopy) as shown in figure 2-10. 176points for closed space and 324 random points for open space were used.

ALS and UAV DTM comparison using 500 random points

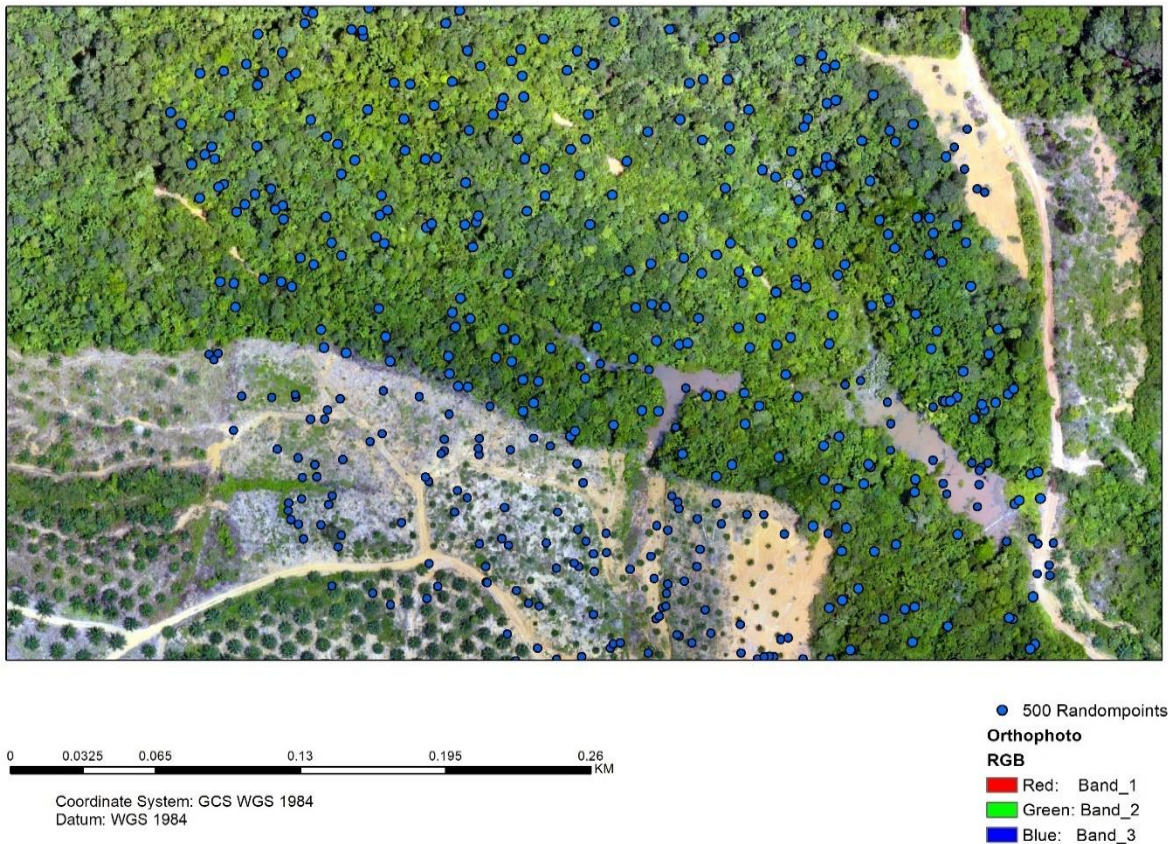


Figure 2-9 500 Random points for comparison of ALS and UAV DTM.



### Open and close space random point

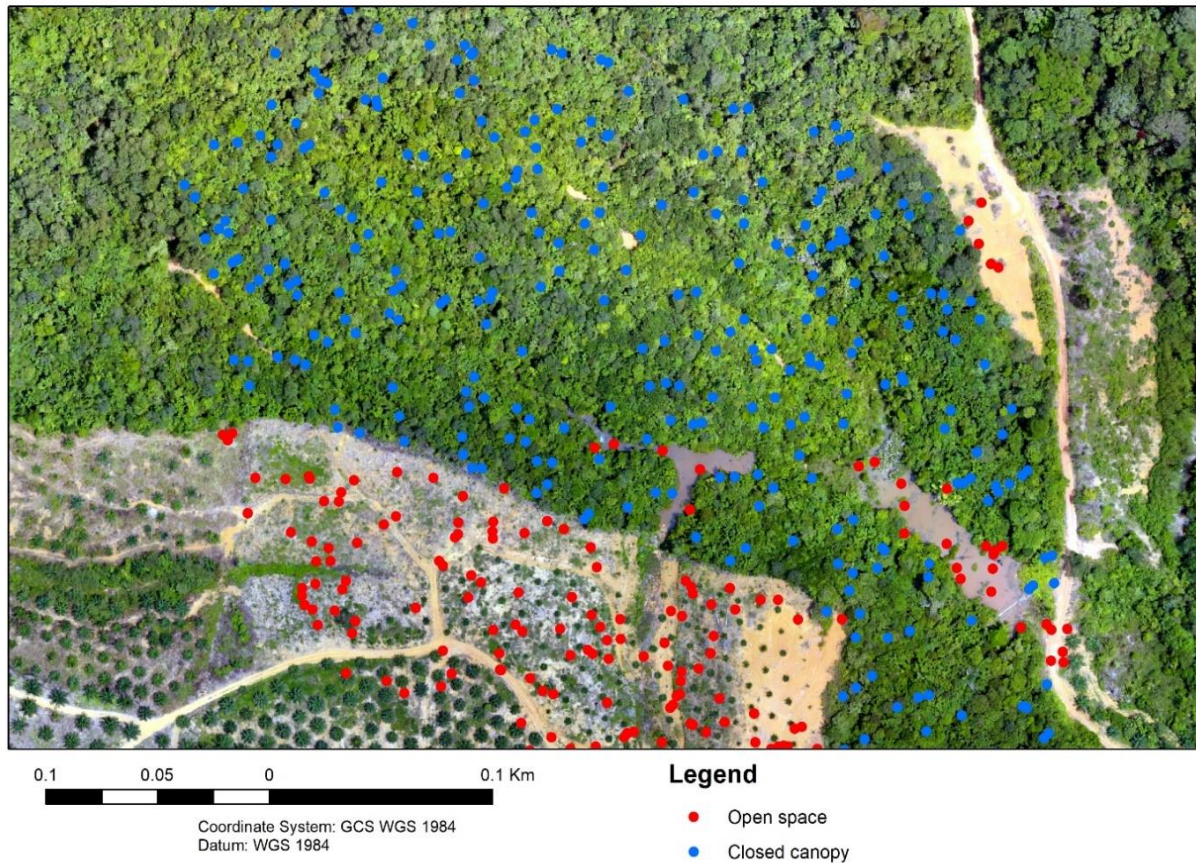


Figure 2-10 Open space and closed space random point for comparison of UAV and ALS DTM.

In this study, a number of statistical analyses were carried out using Microsoft Excel. The regression analysis is the most common method for studying the relationship between two or more variables. Regression test commonly applied in the field of forestry studies to the quantitative relationship and expressed by an equation, regression coefficients, and coefficient of determination (Kahyani et al., 2011). The linear regression and RMSE were used to assess the relationship between UAV DTM and checkpoints (CP) which were measured by DGPS. Also, the biomass/carbon stocks generated by ALS and UAV were analyzed using regression analysis. The t-test was carried out in order to assess whether means of tree height and DTM of ALS and UAV differ significantly.

In this study LiDAR was used to validate UAV tree heights. To assess the effect of tree height difference on AGB, UAV tree heights were used to model LiDAR tree heights based on the root mean square error (RMSE). RMSE was used to assess the deviation of a dependent variable along the line of fit (Equation 2-6).

**Equation 2-6:** Equation for RMSE and %RMSE calculation

$$RMSE = \sqrt{\sum_{i=1}^n \frac{(Y_i - \hat{Y}_i)^2}{n}}$$

Where;

$Y_i$ : -Measured value of the Dependent variable

$\hat{Y}_i$ : -Estimated the value of the dependent variable

$n$ -Number of samples

RMSE-Root Mean Square Error of the relationship

$$\%RMSE = RMSE * n * 100 / \sum Y_i$$

Where;

$Y_i$ : Measured value of the Dependent variable

$\hat{Y}_i$ : Estimated the value of the dependent variable

$n$ : Number of samples

RMSE: Root Mean Square Error of the relationship

%RMSE: Percentage Root Mean Square Error of the Relationship

### 3. RESULT

#### 3.1. DSM, DTM and Orthophoto Generation from UAV images

The DSM, DTM and ortho-mosaic image were generated using Agisoft Photoscan software through the structure from motion technique (SfM). A different number of Ground control points (GCPs) were used to provide spatial referencing of the 3D model and final product of UAV images. A total of 1.7 Km<sup>2</sup> were covered by the three flight blocks where the ortho-mosaic image with ground resolution ranges from 4.53 – 4.98 cm/pixel. Some particular information on the UAV image processing conducted in Agisoft Photoscan is presented in Table 3-1 below. Also, a sample of generated DSM, DTM and ortho-mosaic image are illustrated in figure 3-1 and figure 3-2 below.

Table 3-1 Summary of UAV-image processing report using Agisoft Photoscan Professional.

Area	Mission grid type	Number of used images	Number of used GCP's	Flying Altitude (m)	Coverage Area (Km <sup>2</sup> )	Point density (points/m <sup>2</sup> )	GCP's RMSE (pix)	GSD cm/pix	Resolution cm/pix
1	single	368	4	133	0.4	107	0.2	4.84	9.68
		368	6	133	0.4	107	0.21	4.84	9.68
		368	8	133	0.4	107	0.24	4.84	9.68
		368	10	133	0.4	107	0.31	4.84	9.68
	double	741	4	131	0.4	108	0.22	4.8	9.61
2	single	971	6	129	0.8	108	0.25	4.53	9.07
3	single	470	4	145	0.5	101	0.26	4.98	9.96

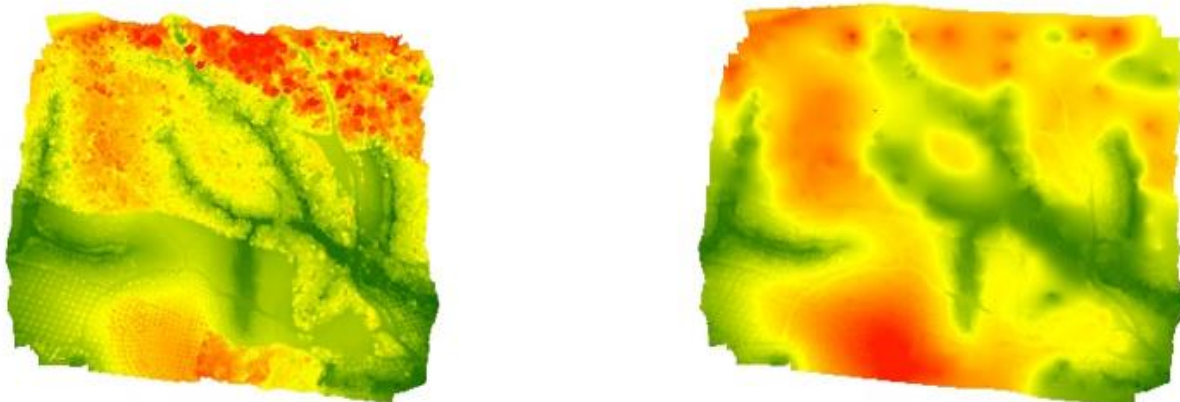


Figure 3-1 UAV DSM and DTM.





Figure 3-2 Small part of the ortho-mosaic image generated from the UAV images.

### **3.2. Comparison of ALS and UAV photogrammetric image matching DTM**

Comparison of ALS and UAV DTM'S which processed with 4, 6, 8 and 10 GCPs (i.e. DTM4, DTM6, DTM8 and DTM 10 ) was a fundamental objective because it has its effect on tree height and consequently on the biomass and carbon stock. ALS DTM was considered to be more accurate under a forest canopy (White et al., 2013). Therefore it was used to assess the accuracy of photogrammetric generated DTM. RMSE, t-test and regression analysis conducted to assess the accuracy of UAV DTM'S Which is explained in this subsection.

#### **3.2.1. Comparison of ALS and photogrammetric image matching DTM'S using Checkpoint recorded by DGPS**

The comparison between UAV DTM'S with different number of GCP'S and ALS DTM was done by using Checkpoint point altitude which was collected by differential GPS. The accuracy of the DGCP was 2 cm and the accuracy assessment of UAV and ALS DTM was assessed using RMSE and RMSE % (Table 3-2 and 3-3)). The accuracy of UAV DTM with 4,6,8 and 10 ground control point, when compared to checkpoint revealed that RMSE of  $\pm 0.9\text{m}$  and RMSE % of 1.6 for all UAV DTM's. The summary of the comparison is shown in Table 3-2 and 3-3. While the relationship of ALS DTM height and Checkpoint is indicated in figure 3-3 and figure 3-4.

Table 3-2 Accuracy assessment of UAV DTMs with different GCPs using Check point collected by DGPS.

UAV DTM Number of GCPs	STATISTICS			
	R <sup>2</sup>	RMSE (m)	RMSE %	Number of CPs
DTM 4	0.98	0.9	1.6	6
DTM 6	0.98	0.9	1.6	6
DTM 8	0.98	0.9	1.6	6
DTM 10	0.98	0.9	1.6	6

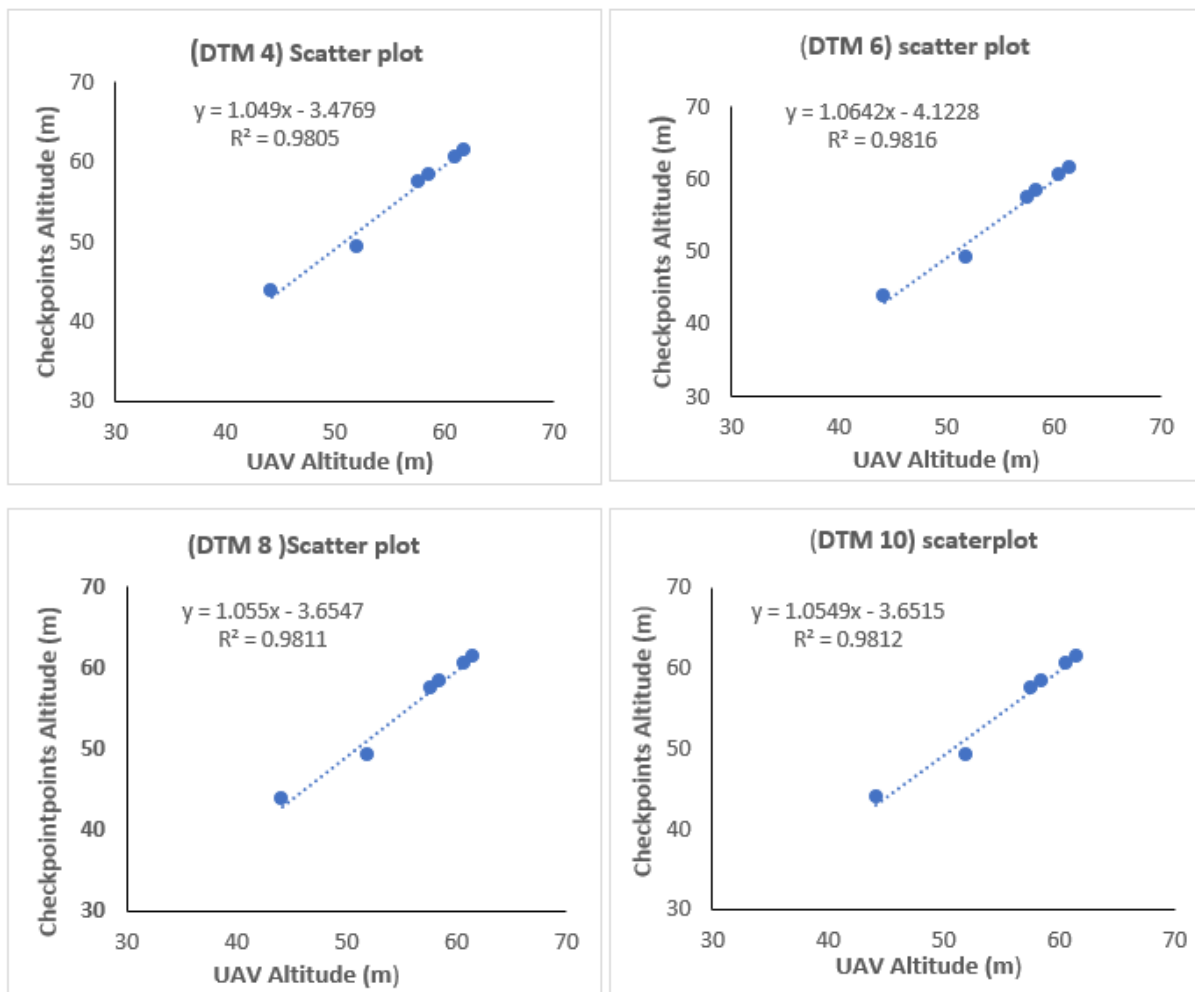


Figure 3-3 Relationship between UAV DTMs with different GCPs and checkpoint height.



Table 3-3 Accuracy assessment of ALS DTM using checkpoint collected by DGPS.

Summary of fit	
R <sup>2</sup>	0.9
RMSE (m)	1.6
RMSE %	3.51

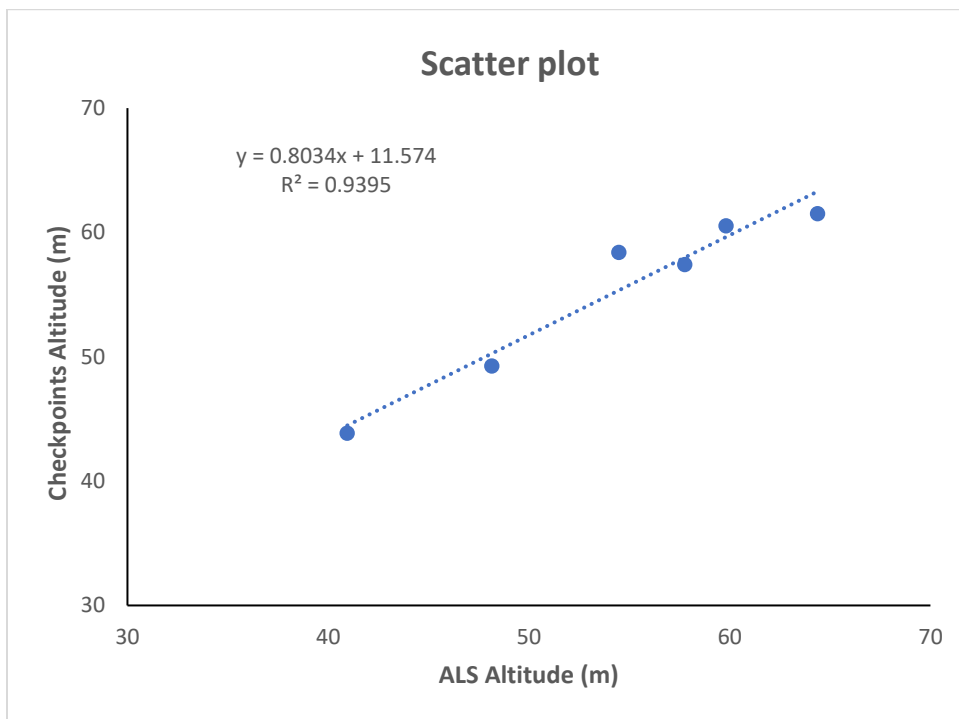


Figure 3-4 Relationship between ALS DTM and Checkpoint height.

### 3.2.2. Comparison of single grid and double grid UAV DTM

In this subsection single grid and double grid UAV photogrammetric image matching DTM with 4 GCP were compared. The t-test analysis was done in order to decide whether to provide and analyze double grid DTM with different number of GCP. For this reason, 500 points were randomly selected using arc map 10.5.1 (Fig 3-5). Then the single and double grid DTM height were extracted using these 500 points. The results (Table 3-4) shows that there is no significant difference between the two DTM where  $t\text{-statistic} < t\text{-critical}$  ( $p < 0.05$ ). The relationship of single and double grid UAV DTM height is indicated in figure 3-6

Table 3-4 The t-test assuming equal variance for UAV single and double grid extracted DTM height.

	Single grid DTM 4	Double grid DTM4
Mean	54.60107214	54.38969154
Variance	36.10579429	34.55783831
Observations	500	500
df	998	
t Stat	0.562279369	
P(T<=t) two-tail	0.574051958	
t Critical two-tail	1.962343846	

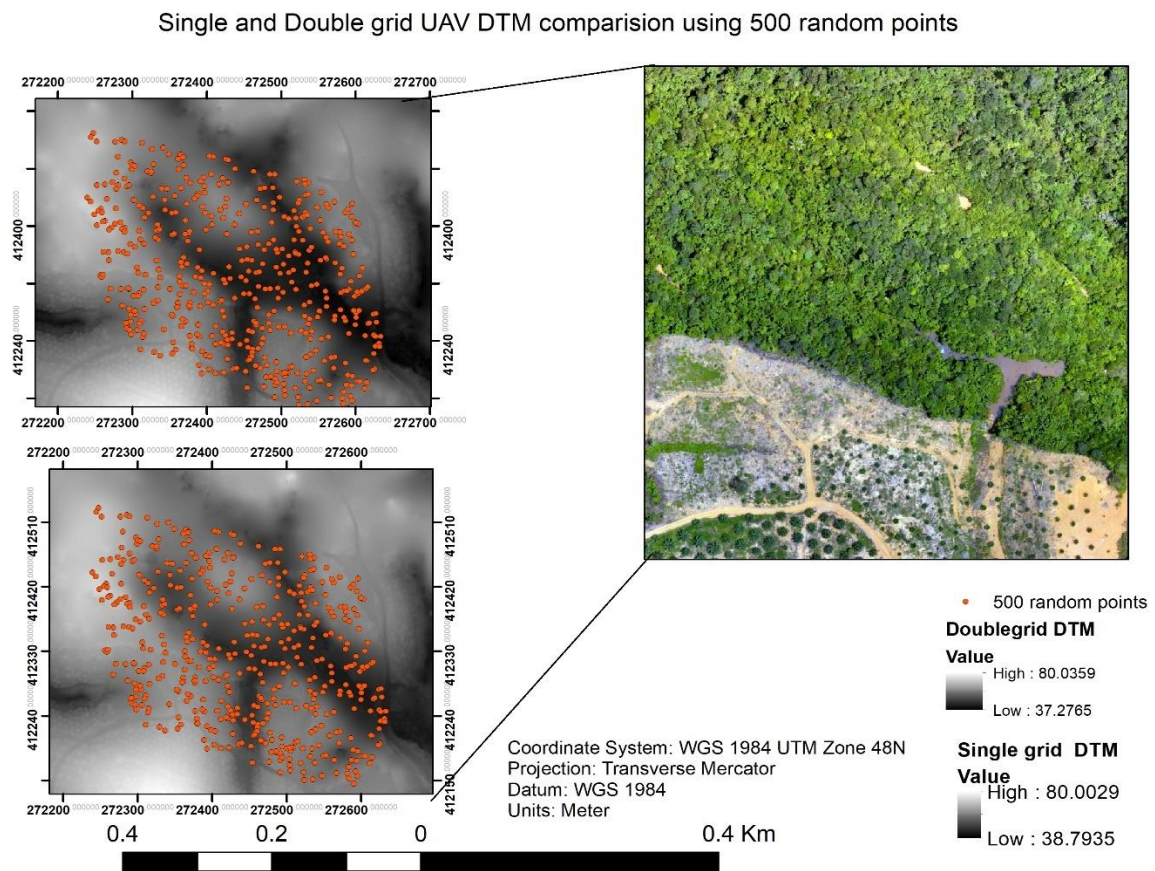


Figure 3-5 Comparison of Single and double grid UAV DTM height based on 500 random points

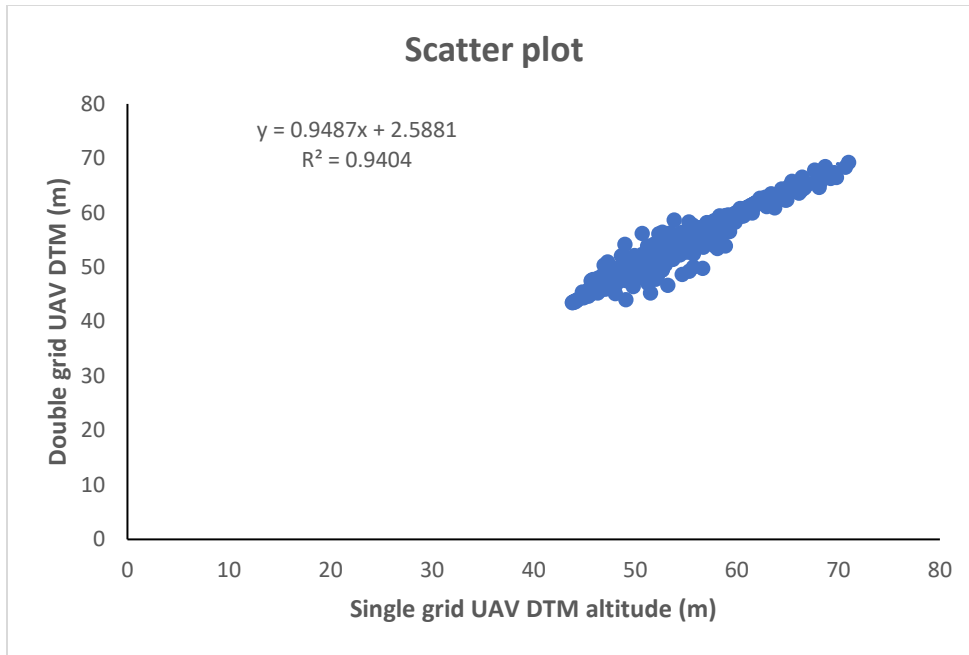


Figure 3-6 Relationship between single and double grid UAV DTM.

### 3.2.3. Comparison of photogrammetric image matching DTM'S and ALS DTM using their height

In this subsection, ALS-DTM and UAV-DTM with different number of GCP were compared. First, the images were co-registered to ensure a perfect spatial match between UAV-DTM and ALS-DTM (figure 3-7). Using Arc-Map 10.5.1, 500 points were generated randomly in the area of interest. Then altitude value of all UAV-DTM'S and ALS-DTM pixels was extracted using these 500 random points. The coefficient of determination ( $R^2$ ), RMSE, RMSE% and t-test (Appendix 3) were carried out the results were summarized in Table 3-5.

Table 3-5 Summary for comparison of ALS-DTM and UAV-DTMs altitude.

Statistics	DTM 4	DTM 6	DTM 8	DTM 10
$R^2$	0.66	0.68	0.67	0.67
RMSE (m)	3.65	3.53	3.51	3.5
RMSE (%)	6.57	6.38	6.33	6.31
n	500	500	500	500

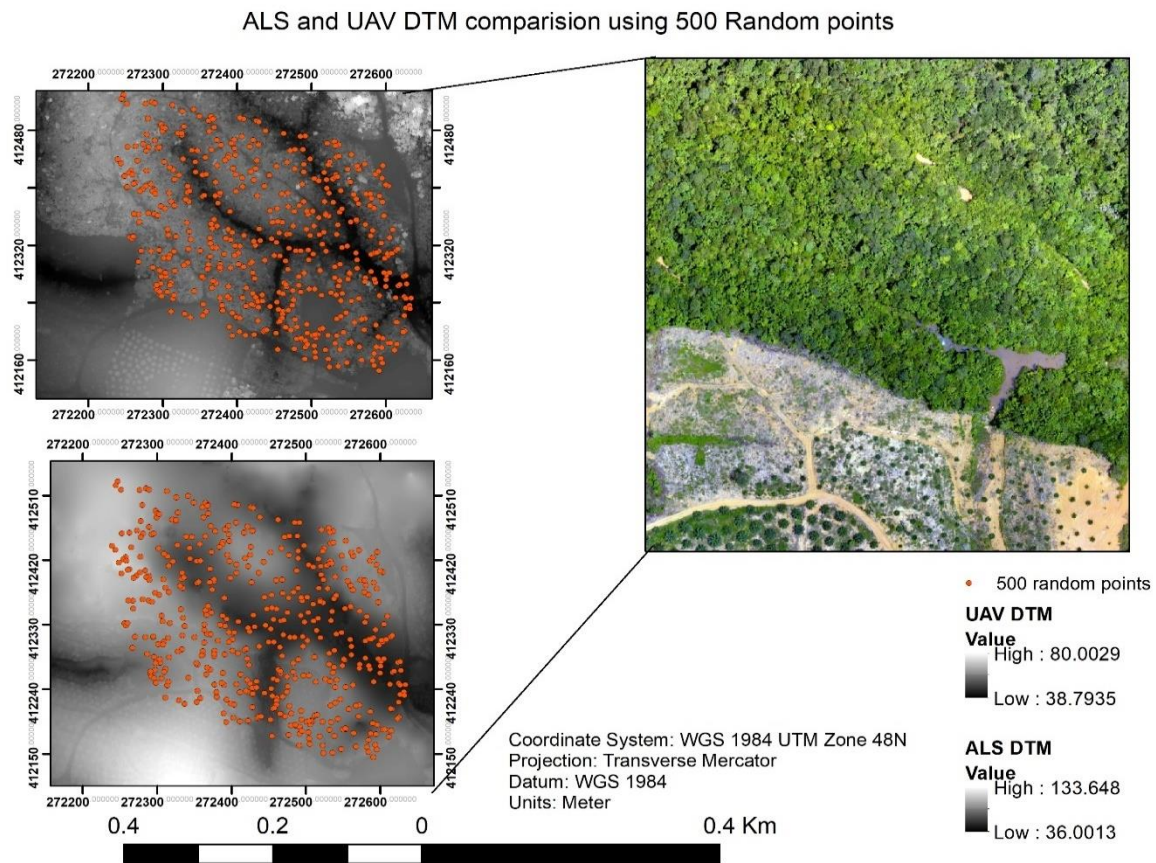


Figure 3-7 Comparison of UAV from ALS DTM height based on 500 random points

Furthermore, UAV-DTMs and ALS-DTM were compared in open terrain and under the closed canopy by grouping the 500 random points into open and closed space (see figure 2-10). The t-test results (Table 3-6) shows that in open space there was no significant difference between all UAV-DTMs with different number of ground control point and the ALS-DTM where  $t\text{-statistic} < t\text{-critical}$  ( $p < 0.05$ ). In the case of closed canopy, there was a significant difference between UAV-DTM with different number of ground control point and ALS-DTM. The coefficient of determination ( $R^2$ ), RMSE, RMSE% and t-test (see Appendix 4) results were summarized in Table 3-7.

Table 3-6 The t-test assuming equal variance for UAV-DTMS and ALS-DTM in open space.

	ALS DTM	DTM 4	ALS DTM	DTM 6	ALS DTM	DTM 8	ALS DTM	DTM 10
Mean	55.2803	55.98014	55.2803	55.73095	55.2803	55.81224	55.2803	55.81262
Variance	46.18783	35.44697	46.18783	36.24936	46.18783	35.87869	46.18783	35.84033
Observations	176	176	176	176	176	176	176	176
df	350		350		350		350	
P(T<=t) one-tail	0.152428		0.255338		0.218256		0.218037	
P(T<=t) two-tail	0.304857		0.510675		0.436512		0.436073	

Table 3-7 Summary for comparison of ALS and UAV DTMs in closed canopy altitude.

Statistics	DTM 4	DTM 6	DTM 8	DTM 10
R <sup>2</sup>	0.67	0.69	0.68	0.68
RMSE (m)	4.1	3.54	3.53	3.49
RMSE (%)	7.4	6.4	6.37	6.31
n	324	324	324	324

### 3.3. CHM Generation from ALS and UAV photogrammetry and segmentation accuracy assessments

The UAV and ALS-CHM were generated by subtracting the DTM from the DSM using the Raster calculator in ArcGIS 10.5.1. The UAV-CHM using the UAV-DTM with 8 GCPs which was relatively the best DTM based on comparison with the ALS-CHM (see Table 3-5 and 3-7). The UAV-CHM is displayed in the 3D view. (figure 3-8).

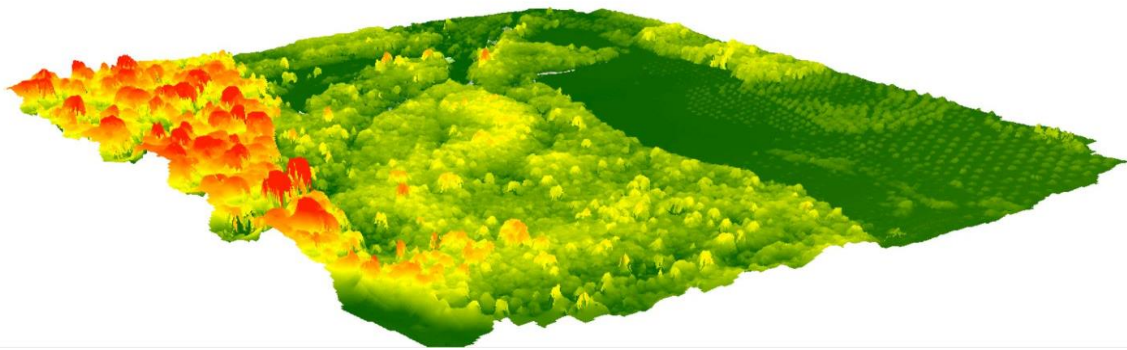


Figure 3-8 UAV Photogrammetry CHM.

Segmentation was done in order to delineate the crown of individual trees. Individual tree identification was important because it was used for matching ALS and UAV estimated tree height. The accuracy of segmentation was assessed by comparing with manually delineated crown polygons. Clearly visible crowns on orthophoto were digitized manually on screen in ArcMap. Manually digitized polygons were then compared with the automatically generated polygons of orthophoto image as shown in figure 3-9. The segmentation goodness (D) value of the 3 areas flown with the UAV ranges from 73 %, 74% and 75% for three flight block respectively. The accuracy was accepted for delineation of the crowns of the individual trees, which were later used for extraction three heights of UAV-CHM and ALS-CHM. The UAV-CHM and ALS-CHM were co-registered to ensure a perfect spatial match. The shapefile with the segmented tree crowns on the UAV-orthophoto was also used to extract the tree height from the ALS-CHM.



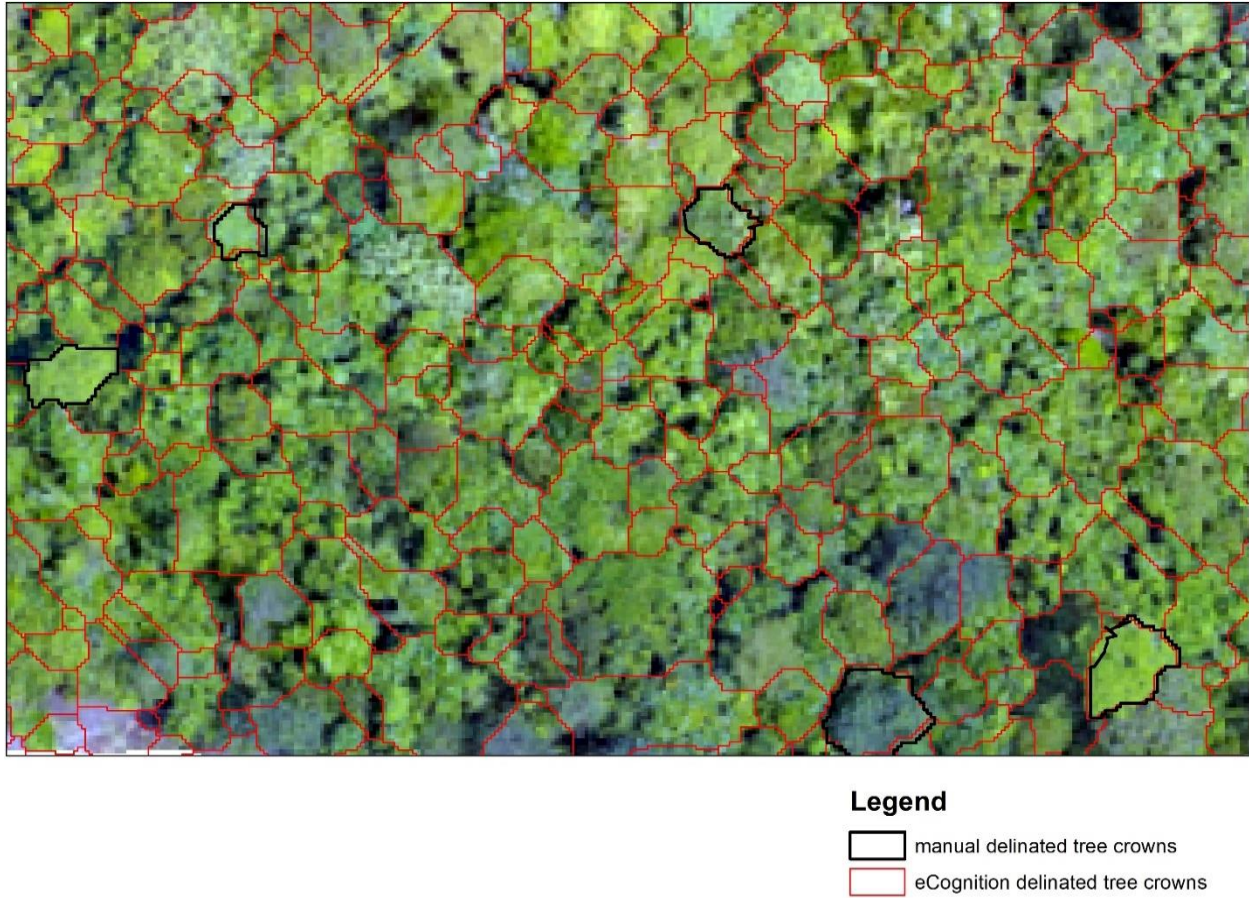


Figure 3-9 Sample showing comparison of manually and eCognition delineated tree crown.

### 3.4. Comparison between the tree heights extracted from UAV-CHM and ALS-CHM

A total of 212 matched trees were used to assess the accuracy of tree heights derived from UAV-CHM (i.e. derived from DTM8) to ALS tree heights. The scatter plot illustrate the relationship between the UAV-CHM and ALS-CHM extracted heights (figure 3-10) coefficient of determination ( $R^2$ ) of 0.605. The root mean square error (RMSE) was  $\pm 2.1\text{m}$  which are equivalent to 24% of the total estimated tree height from UAV-CHM (Table 3-8).

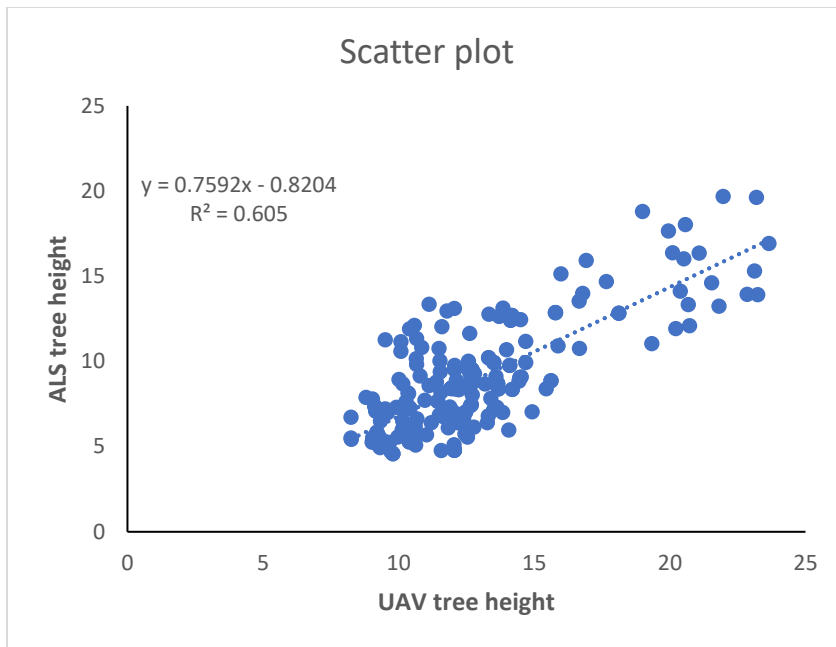


Figure 3-10 The scatter plot of ALS-CHM and UAV-CHM extracted tree height.

Table 3-8 Summary for comparison of ALS and UAV tree heights.

Statistics	
R square	0.60
RMSE(m)	2.18
RMSE%	24.37
Observation	212

Furthermore, The F-test was conducted to find out if the two samples (ALS-CHM and UAV-CHM tree heights) have an equal variance or unequal variance, in order to determine which t-test to use to detect the difference between the two methods. The results of the F-test shows equal variance between the two samples see Table 3-9 where the F-statistic < F-critical ( $P > 0.05$ ). Therefore a t-test assuming equal variance was conducted.

Table 3-9 F-test of two samples for variance.

	ALS	UAV
Mean	8.954264	12.87427206
Variance	10.40554	10.92142691
Observations	212	212
df	211	211
F	0.952764	
P(F<=f) one-tail	0.362792	
F Critical one-tail	0.796934	

To find out if there is a significant difference between the tree heights extracted from UAV-CHM and ALS-CHM a t-test assuming equal variance was conducted. The results (Table 3-10) shows that there is a significant difference between UAV-tree height and ALS-tree height where t-statistic > t-critical ( $p < 0.05$ ).

Table 3-10 The t-test assuming equal variance for ALS and UAV extracted tree height.

	ALS Tree height	UAV Tree height
Mean	8.954264047	12.87427206
Variance	10.40553968	10.92142691
Observations	212	212
df	422	
t Stat	-12.35919945	
P(T<=t) one-tail	1.83592E-30	
t Critical one-tail	1.648472442	
P(T<=t) two-tail	3.67183E-30	
t Critical two-tail	1.965601364	

### 3.4.1. Comparison of tree heights extracted from UAV-CHM, and ALS-CHM in areas where the DTMs are nearly the same.

The quality of the DTM is influenced by the density of the points at terrain level and the CHM and subsequent tree height are directly depending on the DTM. In areas with a closed canopy, the differences in ALS-DTM and UAV-DTM are expected to be larger. For this reason, 154 trees, 60 trees from first flight block, 18 trees from second flight block and 76 trees from the third flight, were selected in areas where there was a small difference in altitude between ALS-DTM and UAV-DTM and the tree heights were compared using t-test.

The results indicated that the mean tree height measured by ALS was 14.5 m with a standard deviation of 5.8. While mean of UAV estimated trees height was 15.53 m with a standard deviation of 6.45m. The detailed summary statistics of the tree height estimated by UAV and ALS was shown in Table 3-11.



Table 3-11 Descriptive statistics of the ALS and UAV measured tree height in the area where DTMs have slightly difference.

	ALS Tree height	UAV Tree height
Mean	14.50930169	15.53643511
Standard Error	0.47417898	0.520408701
Standard Deviation	5.884406394	6.458102146
Sample Variance	34.6262386	41.70708333
Range	32.86878204	29.53923035
Minimum	5.192390442	6.044624329
Maximum	38.06117249	35.58385468
Sum	2234.432461	2392.611008
Count	154	154

Furthermore, the relationship between ALS-CHM and UAV-CHM tree heights was established in order to assess how well UAV-tree heights can predict ALS tree heights. The scatter plot illustrate the relationship between the UAV-CHM and ALS-CHM extracted heights (figure 3-11) coefficient of determination ( $R^2$ ) of 0.88. The root mean square error (RMSE) was  $\pm 2.4$  m which are equivalent to 13% of the total estimated tree height from UAV-CHM (Table 3-8).

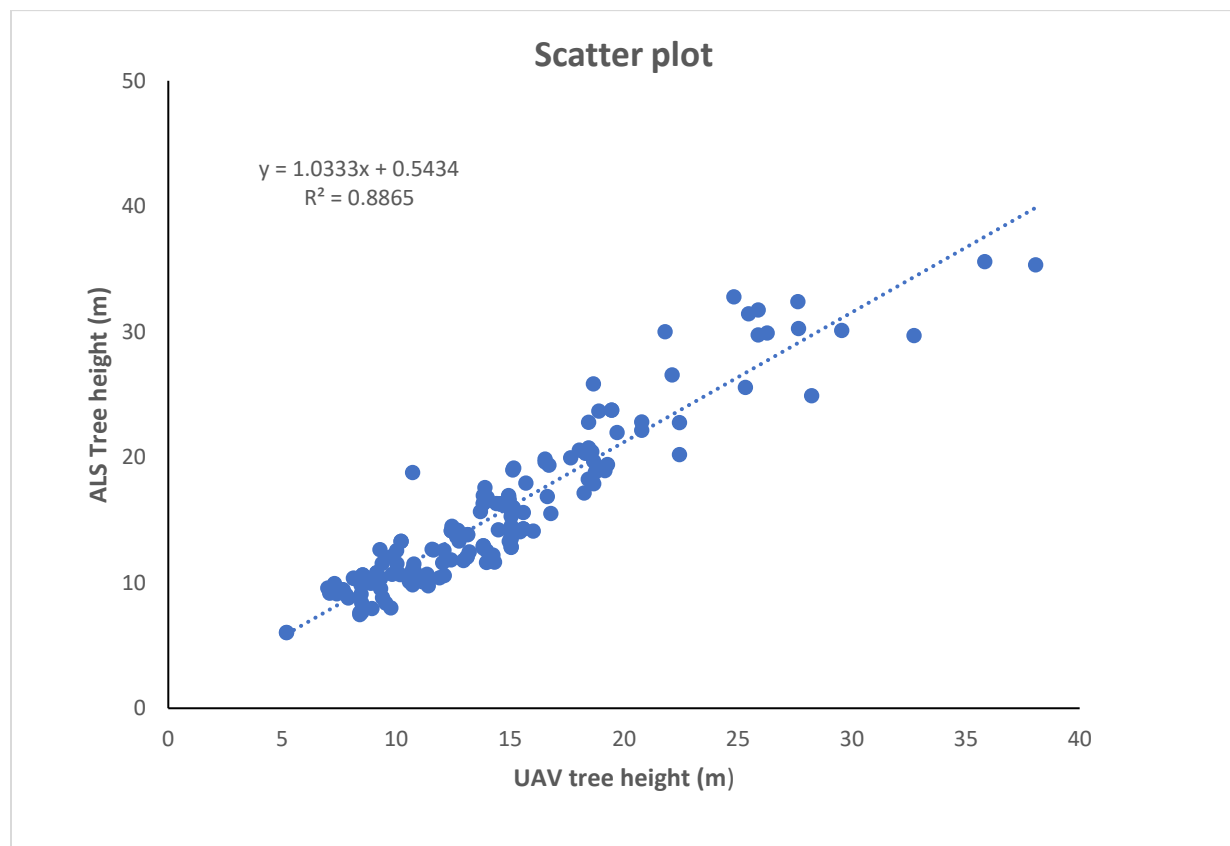


Figure 3-11 The scatter plot of ALS-CHM and UAV-CHM extracted tree height in areas where the DTMs are nearly the same.

Table 3-12 Summary for comparison of ALS and UAV tree heights in areas where the DTMs are nearly the same.

statistics	
R square	0.88
RMSE(m)	2
RMSE%	13
Observation	154

The F-test was conducted to find out if the two samples (ALS-CHM and UAV-CHM tree heights) have an equal variance or unequal variance, in order to determine which t-test to use to detect the difference between the two methods. The results of the F-test shows equal variance between the two samples (Appendix 5) where the F-statistic < F-critical ( $P > 0.05$ ). Therefore a t-test assuming equal variance was conducted. The results (Table 3-13) shows that there is no significant difference between the two methods where t-critical > t-statistics ( $p < 0.05$ ).

Table 3-13 The t-test assuming equal variance for ALS and UAV extracted tree height in areas where the DTMs are nearly the same.

	ALS Tree height	UAV Tree height
Mean	14.50930169	15.53643511
Variance	34.6262386	41.70708333
Observations	154	154
df	306	
t Stat	-1.458915505	
P(T<=t) one-tail	0.072807033	
t Critical one-tail	1.649848466	
P(T<=t) two-tail	0.145614066	
t Critical two-tail	1.967746738	

### 3.5. Biometric data

In this study DBH and XY coordinates were collected as biometric data. The following section describe the detail of descriptive statistic of DBH calculated by Microsoft excel.

#### Diameter at Breast Height (DBH)

Diameter at breast height was collected in 13 plots in, a total of 600 trees were recorded while total of 212 trees were matched (Appendix 6) between ALS and UAV . The descriptive statistic on DBH was carried out using Microsoft excel. The mean tree DBH of 11.81 cm was recorded. The summary of the descriptive statistics is shown in Table 3-14.

Table 3-14 Descriptive statistics of DBH height.

DESCRIPTIVE	
Mean DBH [cm]	11.81
Standard Error (cm)	0.37
Standard Deviation [cm]	5.34
Minimum DBH [cm]	5
Maximum DBH [cm]	35
Total number of Matched trees	212

### 3.5.1. Controlled Field experiment

Ten trees were selected in undulating terrain in which UAV camera unable to image the ground (see figure 3-8). Then accuracy of UAV tree height estimation was assessed by ALS Tree heights. The accuracy assessment of selected Trees height of UAV by ALS tree height revealed that RMSE of  $\pm 5.1$  (Appendix 7) meter which are equivalent to 16% of the total estimated tree height from UAV-CHM.

### 3.6. Biomass and carbon estimation

The amount of biomass of the trees was calculated using an allometric equation. Tree height estimated from first flight block using UAV-CHM and ALS-CHM, DBH and default wood density value of  $0.57 \text{ g/cm}^3$  was used for AGB computation. The total Biomass of 212 trees was 10.63 Mg for ALS and 15.41 Mg for UAV estimated tree height. The summary of descriptive statistics (Table 3-14) and relationship in regression line (Appendix 8) and accuracy of UAV biomass is shown in Table 3-15.

Table 3-15 Descriptive statistics for ALS and UAV biomass.

Statistics	ALS	UAV
Mean Biomass [Mg] per tree	0.05	0.07
Standard Deviation	0.07	0.10
Minimum biomass (Mg) per tree	0.01	0.01
Maximum Biomass (Mg) per tree	0.47	0.76
Total biomass of 212 trees	10.63	15.41
Observation (Total Trees)	212	212

Table 3-16 Summary of relationship and accuracy of UAV computed Biomass.

statistics	
R square	0.93
RMSE(Mg)	0.02
RMSE%	33
Observation	212

Furthermore, Carbon stock of the trees was estimated based on a conversion factor of 0.47 of the calculated biomass. The descriptive statistics indicated that in the total matched trees 212 the average mean carbonstock of ALS and UAV was 0.023 and 0.034 Mg respectively. The summary of descriptive statistics is shown in Table 3-16 and relationship regression line (Appendix 9) and accuracy of the UAV carbon stock is shown in Table 3-17.

Table 3-17 Descriptive statistics for ALS and UAV carbon stock.

Statistics	ALS	UAV
Mean Carbon Stock [Mg] per tree	0.0235	0.0341
Standard Deviation	0.0312	0.0451
Minimum Carbon stock per trees	0.0023	0.0041
Maximum Carbon stock per trees	0.2210	0.3549
Total Carbon stock [Mg] of 212 trees	4.997	7.2417
Observation (Total Trees)	212	212

Table 3-18 Summary of relationship and accuracy of UAV computed carbon stock.

statistics	
R square	0.93
RMSE(Mg)	0.07
RMSE%	33
Observation	212

### 3.7. Comparison of UAV-AGB and ALS-AGB

To reveal the effect of differences of tree height estimation on the AGB a total of 30 trees were selected randomly from first, second and third flight block. Tree height of 30 trees estimated from UAV-CHM and ALS-CHM, DBH and default wood density value of 0.57 g/cm<sup>3</sup> was used for AGB computation. Then, F-test

was conducted to find out if the two samples (ALS computed AGB and UAV-Computed AGB) have an equal variance or unequal variance, to determine which t-test use to detect the effect of ALS and UAV tree height difference on AGB. The results of the F-test shows equal variance between the two samples (see Appendix 10) where the F-statistic < F-critical ( $P > 0.05$ ). Therefore a t-test assuming equal variance was conducted. The results (Table 3-19) shows that there is no significant difference between the two computed AGB where  $t\text{-critical} > t\text{-statistics}$  ( $p < 0.05$ ).

Table 3-19 The t-test assuming equal variance for UAV and ALS computed AGB.

	ALS AGB	UAV AGB
Mean AGB (Mg) per tree	0.0494242	0.054409341
df	58	
t Stat	-0.30	
P(T<=t) one-tail	0.38	
t Critical one-tail	1.67	
P(T<=t) two-tail	0.76	
t Critical two-tail	2.00	

On the other hand, The relationship between tree height estimated by UAV and ALS indicated that RMSE of  $\pm 2$  m. Thus, the RMSE was used as a basis to assess the effect of differences of trees height measurements on AGB. It was done by adjusting the UAV trees height based on the potential RMSE obtained and realize how it was affecting the AGB. Thus, the effect of differences of trees height measurements in the AGB of random selected thirty (30) trees was plotted by adjusting the value of tree height in the range of -2 m to +2 m due to RMSE of  $\pm 2$  m (see Table 3-20 and figure 3-12).

Table 3-20 Effect of differences of measured field tree height on biomass estimation.

Statistics	RMSE[-2]	RMSE[-1]	RMSE[0]	RMSE[+1]	RMSE[+2]
Mean biomass [Mg] per tree	0.04	0.05	0.05	0.06	0.06
Standard Deviation	0.06	0.06	0.07	0.07	0.08
Range	0.29	0.33	0.36	0.40	0.43
Minimum biomass [Mg] per tree	0.01	0.01	0.01	0.01	0.02
Maximum biomass [Mg] per tree	0.30	0.34	0.37	0.41	0.45
Total biomass [Mg] of 30 trees	1.34	1.49	1.63	1.78	1.92
Selected trees	30	30	30	30	30

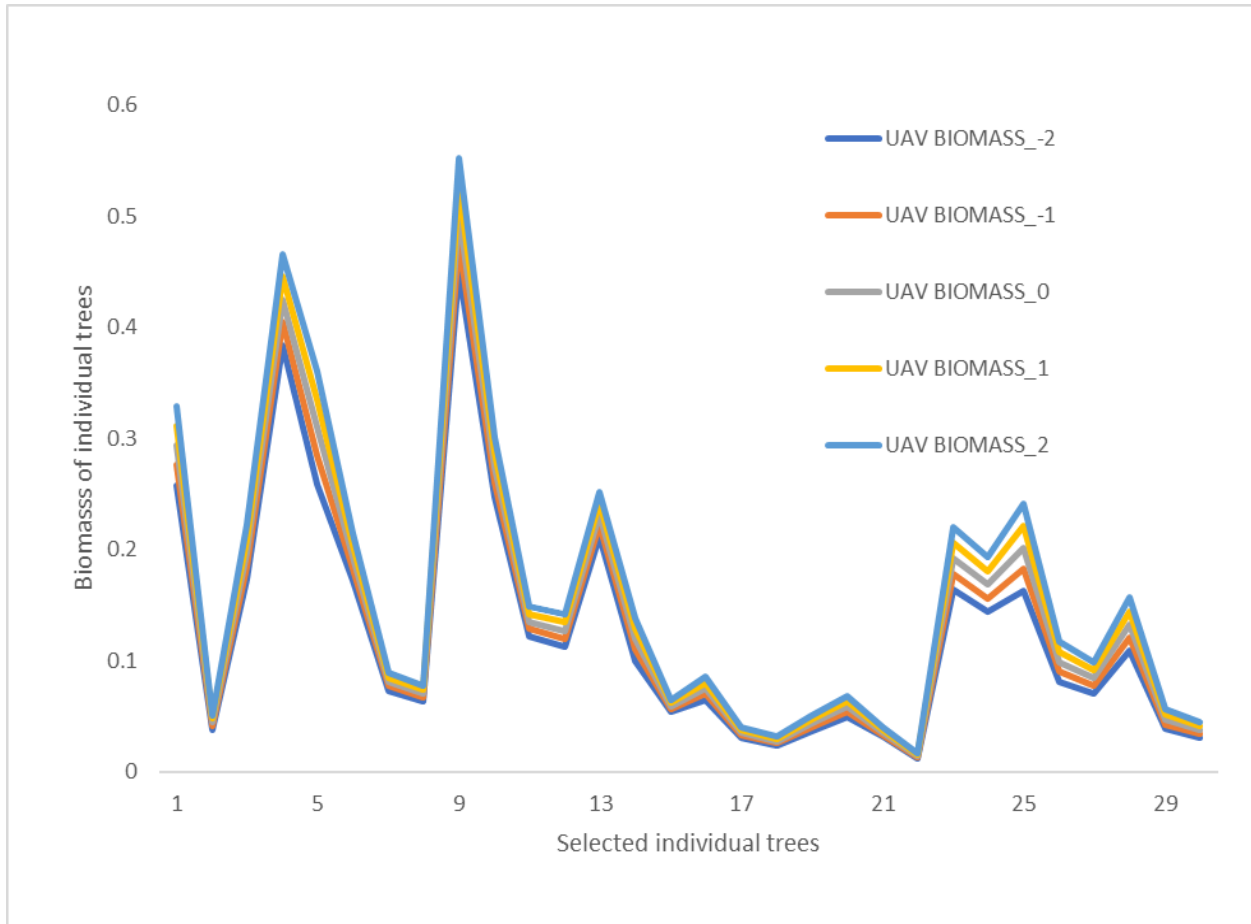


Figure 3-12 Effect of differences of field measured tree height on AGB estimation.

## 4. DISCUSSION

### 4.1. Accuracy of UAV DTM with different number of Ground control point

In this study, DTM of UAV imagery with different number of GCP'S number of GCPs was derived. The flight altitude was 120 m, the side overlap 60-70% and front overlap 90%. These parameters influence the quality of a DTM generated from UAV images. The study by Carrascosa et al. (2016) emphasizes that increase in the percentage of side and front overlap reduces error in positional accuracy. Higher overlap increases the number of extracted tie points, which positively affects the quality of the DTM.

The accuracy of UAV-DTM with different number of GCPs and ALS DTM was assessed by Checkpoints. The result revealed that  $R^2$  of 0.98 for DTM4, DTM6, DTM8 and DTM 10 With RMSE of  $\pm 0.9$ . while ALS DTM had  $R^2$  of 0.90 with RMSE of  $\pm 1.5$  m. When comparing the RMSE of UAV-DTM'S and ALS-DTM it becomes clear the UAV-DTM performs better than the ALS-DTM. This may be due to point density difference, UAV has 106 points/m<sup>2</sup> while ALS with 5 points/m<sup>2</sup>.

These results contradict with Reuben (2017). When comparing to (checkpoints) DGPS, the UAV-DTM performs better than ALS-DTM indeed due to a higher point density. On the other hand, Reuben (2017) results revealed that ALS DTM Better than UAV DTM compared to (Checkpoint) DGCP point. If the claim of Reuben (2017) was correct, the UAV-DTM in open spaces to be similar to the ALS-DTM. That is not the case.

The Accuracy assessment result of UAV DTM by ALS DTM (RMSE  $\pm 3$  m up to  $\pm 4.05$  m) of Reuben (2017) was very close to the results of this study (RMSE  $\pm 3.5$ m up to  $\pm 3.65$ m) when the comparison made using all 500 random points. It could very well because of the error in the ALS-DTM. Although the ALS accurately measure the tree height (Andersen et al., 2006) while the UAV estimates the tree height, both systems are hampered by the fact that the canopy limits the information obtained from the forest floor. It all boils down to the density of the point cloud on which the DTM is constructed. The larger the number of points, the better the DTM (Estornell, Ruiz, Velázquez-Martí, & Herмосilla, 2011). This is in line with this study result where UAV DTM performs better than ALS DTM in comparison to Checkpoints due to the number of point density.

This study also goes further and compare UAV DTM in the open space and closed canopy by classifying 500 random points into open and closed ( see fig 3-7). The t-test assuming equal variance shows that there was no significant difference between UAV-DTM and ALS-DTM in open space (Bare land ). On the other hand in closed canopy (densely vegetated area) RMSE of  $\pm 4.1$ ,  $\pm 3.54$ ,  $\pm 3.53$ ,  $\pm 3.49$  for DTM4, DTM6, DTM8 and DTM10 respectively. The reason for high RMSE was due to the fact that UAV Camera was not able to image the ground. This result in missing information in the ground and form DTM by interpolation for closed canopy ground surface.

A similar study was conducted by Debella-Gilo & Iii, (2016) in which different UAV DTM generated using different interpolation method in four sites including bare area and undulating area with dense forest. RMSE was used to assess the accuracy of UAV DTM. The RMSE of bare land lower than dense forest area (Table 4-1) which is very close to the result with this study.

Table 4-1 The RMSE error variables of the DTMs interpolated by the four different methods for the two test sites.

Interpolation method	RMSE	Bare area	Dense forest+ open areas
Inverse distance Weighted	RMSE	0.7	2.4
	Standard error	0.7	2.3
Natural Neighbor	RMSE	0.6	2.2
		0.5	1.1
Regular spline	RMSE	0.7	2.5
	Standard error	0.5	1.3
ANDUEM	Standard error	0.5	2.1

Source: (Debella-Gilo & Iii, 2016)

#### 4.2. Source of Tree height variation by UAV photogrammetry

This study shows that UAV tree height is not significantly different from ALS tree height in areas where the DTMs are nearly the same. For the main study area (first flight block) flight, there are significantly different between ALS and UAV tree heights with RMSE of  $\pm 2$  meters. The error was due to that in a very dense area UAV unable to image the ground thus interpolation made from the open area. The undulating area was not characterized correctly which result in an error in tree heights of UAV. The error from UAV tree height is depicted in trees which collected in steep slope and undulating terrain in flight block 2. Ten tree was selected in undulating terrain in which UAV camera unable to image the ground (see Fig 2-8). Then accuracy of UAV tree height estimation was assessed by ALS Tree heights.

The accuracy assessment of selected Trees height of UAV by ALS tree height indicates that RMSE of  $\pm 5.1$  m (Appendix 6) which are equivalent to 16% of the total estimated tree height from UAV-CHM. The error from UAV tree height is attributed to the inaccuracy of the terrain model from UAV-DTM. This result was comparable to the study done by Reuben (2017) in Ayer Hitam forest where he reported that RMSE of  $\pm 3.65$ m in flight six block. As he explained in his study the UAV point cloud unable to penetrate the ground to characterize the ground terrain which results in inaccuracy in tree height Estimation.

#### 4.3. UAV Tree height Estimation

In total, 212 matched trees were estimated by UAV-CHM (i.e. derived from DTM8). The mean tree height estimated was 12.91 with the standard deviation of  $\pm 3.3$  m and trees height was ranging from 8 m to 23.6m minimum and maximum respectively. Next the UAV tree height is compared with tree heights of ALS. When UAV tree height was regressed with ALS derived tree height,  $R^2$  of 0.6 was obtained. This indicated that the variation in tree height estimated by UAV was explained by ALS tree height by 60%.



The accuracy assessment of UAV tree height was evaluated by using tree height derived from ALS and the RMSE of  $\pm 2.18$  (RMSE=24.37%) was obtained. On the other hand t-test assuming equal variance was computed and shows that there was a significant difference between UAV and ALS DTM (Table 3-10). This study is comparable to the study conducted by Reuben (2017) in which in his study 388 trees matched between tree heights of ALS and UAV. The study revealed that  $R^2$  of 0.62 and RMSE of 2.45 when UAV tree height assessed by ALS tree height.

Furthermore, this study compares tree heights of UAV and ALS in areas with a small difference in altitude between ALS-DTM and UAV-DTM. A total of 154 trees from three flight block were used to assess the quality of UAV-CHM in comparison to ALS-CHM. The result revealed that  $R^2$  of 0.88 and RMSE of  $\pm 2.1$  (RMSE =13%). This indicated that the variation in tree height estimated by UAV was explained by ALS tree height by 88%. There was a strong relation between UAV tree height and ALS Tree height. The t-test revealed that there was no significant difference between UAV and ALS tree height since it was derived in areas where the DTMs are nearly the same. The study conducted by Wallace (2016) is comparable to this result. The study indicates that  $R^2$  of 0.68 with RMSE of  $\pm 1.3$  in comparison to UAV tree heights with ALS tree height.

#### **4.4. Estimation of above ground biomass and carbonstock**

The general allometric equation by developed by Chave et al. (2014) was used. The equation uses DBH, tree height and wood density as an input to compute AGB. The use of generic allometric equation in a tropical forest is suitable due to that the equation developed using a large number of trees from different regions (Chave et al., 2005; Gibbs et al., 2007).

To get the input to the allometric equation such as tree height and DBH identification of the individual trees was done using the coordinates of the trees as recorded in the field and segmented image. Due to the error in the GPS measurements, this was not a perfect fit, and the final step was to visually compare the pattern of the coordinates as recorded in the field with the pattern of the segmented tree crowns in order to determine which segment belongs to which individual tree in the field. This tree matching error is one of the sources of error on AGB calculations using ALS and UAV.

For the total of 212 matched trees, the total amount of biomass computed from ALS was 10.63 Mg and 15.41 Mg for UAV. This result contradicts with the result of Reuben (2017) which reported the AGB of ALS and UAV 189.48 Mg and 177.13Mg respectively for 388 trees. The lower in the amount of AGB is due to that the study area is characterized by young trees (see section 2.4.2). The relationship between ALS and UAV GB show that  $R^2$  of 0.93 and RMSE of 0.02 Mg. The  $R^2$  indicated that 93% of AGB of UAV was explained by ALS.

Carbon stock of UAV and ALS was computed using a conversion factor of 0.47. The total amount of carbon stock computed from ALS was 4.997Mg and 7.2417Mg for UAV.

#### **4.5. Effect of differences of UAV and ALS tree height on biomass**

A comparison was made, based on a root-mean-squared error, between UAV tree height and ALS tree height. The RMSE was  $\pm 2$  m which are equivalent to 13% of the total estimated tree height from UAV-CHM. To assess the effect of differences of trees height measurements on AGB, a scatter plot of random selected thirty (30) trees were plotted by adjusting the value of tree height in the range of -2 m to +2 m due to RMSE of  $\pm 2$  m (see figure 3-12). The above ground biomass estimated using allometric equation by Chave et al (2014) and ranges from 0.01Mg-0.45 Mg per tree for randomly selected 30 trees. Further more t-test conducted and the

result revealed that This indicates that there is no significant difference between the two computed AGB (see Table 3-19). .AGB is not affected by tree height since the allometric equation by Chave et al (2014) entails that tree height has little contribution to AGB when compared to DBH.

#### **4.6. Limitation**

- ✓ Handled GPS error was Limitation for tree matching process for tree height comparison and AGB estimation. This is one of the sources of error for AGB calculation.
- ✓ The difference in data acquisition time between UAV and ALS may be the source of error for tree height comparison.
- ✓ Data processing of UAV images consumed time which generated point clouds, DSM and DTM.
- ✓ The flying height of UAV which has an effect on UAV DTM restricted by aviation regulation.

## 5. CONCLUSION AND RECOMMENDATION

### 5.1. Conclusion

What is the accuracy of DTM derived from UAV in relation to number and layout of GCPs in comparison to the DTM derived from Airborne LiDAR?

The UAV DTM and ALS DTM were assessed by Checkpoint recorded by DGPS. The  $R^2$  of 0.9806, 0.9816, 0.9811 and 0.9805 and RMSE of 0.9m, 0.8m, 0.8m and 0.8m were achieved for DTM4, 6, 8, and 10 respectively. The accuracy of ALS DTM, when compared to the checkpoint, achieved an  $R^2$  of 0.93 and RMSE of 1.9m. The accuracy of ALS DTM was less than UAV because of the difference in point density and time of acquisition of UAV and LiDAR data. Furthermore, the accuracy of UAV DTM with different number of ground control point when compared to ALS DTM achieved an RMSE of  $\pm 4.1m$ ,  $\pm 3.54m$ ,  $\pm 3.53m$  and  $\pm 3.49m$  for DTM4, DTM6, DTM8 and DTM 10 respectively. The t-test revealed that there was a significant difference between the DTM of ALS and UAV DTM. Hence The null hypothesis was rejected.

What is the accuracy of tree heights derived from the UAV based CHM in comparison to tree heights derived from the LiDAR based CHM?

The accuracy of tree height estimated from UAV assessed by ALS tree height since ALS provides an accurate DTM. The tree height derived from UAV compared to ALS tree height in relatively closer altitude. The result showed that  $R^2$  of 0.88 and RMSE of  $\pm 2.1m$ . The t statistics showed that there was no significant difference between the two measurements. On the other hand, the tree height derived in the entire area using best UAV DTM (DTM8) was assessed by ALS tree height. The result revealed that tree height was estimated by the accuracy of 80.9% (RMSE= $\pm 2.5$  m, RMSE%=19.07 and  $R^2=0.50$ ). The t-statistics result showed that there was a significant difference between the two measurements. Therefore, The null hypothesis was rejected.

How are AGB and carbon stocks estimates affected by tree height difference between UAV and LiDAR based data?

ALS tree height and UAV tree height was used to estimate biomass and carbon stock. The RMSE of UAV tree height, when validated by ALS tree height, was used to adjust UAV tree height. Then AGB and carbon stock estimated from the adjusted tree height. The t-statistics result showed that there was no a significant difference between ALS AGB and UAV AGB. Therefore, The null hypothesis was not rejected

### 5.2. Recommendation

The GPS receiver used for this study had an error due to the closed canopy of a forest. This made difficulties in tree matching process. Therefore it is recommended to use Differential GPS to record the plot centre to make easier for tree matching process for other studies in tropical forests.

Since the UAV photogrammetric unable to characterize the terrain inside the closed canopy and result inaccurate estimation of tree height. It is recommend to use UAV LiDAR for future other studies.

## LIST OF REFERENCES

- Agisoft. (2017). Dense Cloud Classification & DTM Generation. Retrieved August 9, 2017, from <http://www.agisoft.com/index.php?id=35>
- Andersen, H.-E., Reutebuch, S. E., & McGaughey, R. J. (2006). A rigorous assessment of tree height measurements obtained using airborne lidar and conventional field methods. *Canadian Journal of Remote Sensing*, 32(5), 355–366. <https://doi.org/10.5589/m06-030>
- Bazew, N. M. (2017). Integrating Airborne Lidar and Terrestrial Laser Scanner Forest Parameters for Accurate Estimation of Above-Ground Biomass/Carbon in Ayer Hitam Tropical Forest Reserve, Malaysia, #61. Retrieved from [http://www.itc.nl/library/papers\\_2017/msc/nrm/bazew.pdf](http://www.itc.nl/library/papers_2017/msc/nrm/bazew.pdf)
- Böttcher, H., Eisbrenner, K., Fritz, S., Kindermann, G., Kraxner, F., Mccallum, I., & Obersteiner, M. (2009). An assessment of monitoring requirements and costs of “Reduced Emissions from Deforestation and Degradation.” *CarCarbon Balance and Management*, 4(7). <https://doi.org/10.1186/1750-0680-4-7>
- Boudreau, J., Nelson, R. F., Margolis, H. A., Beaudoin, A., Guindon, L., & Kimes, D. S. (2008). Regional aboveground forest biomass using airborne and spaceborne LiDAR in Québec. *Remote Sensing of Environment*, 112(10), 3876–3890. <https://doi.org/10.1016/J.RSE.2008.06.003>
- Brown, S. (2002a). Measuring carbon in forests: current status and future challenges. *Environmental Pollution*, 116(3), 363–372. [https://doi.org/10.1016/S0269-7491\(01\)00212-3](https://doi.org/10.1016/S0269-7491(01)00212-3)
- Brown, S. (2002b). Measuring carbon in forests: current status and future challenges. *Environmental Pollution*, 116(3), 363–372. [https://doi.org/10.1016/S0269-7491\(01\)00212-3](https://doi.org/10.1016/S0269-7491(01)00212-3)
- Chave, J., Andalo, C., Brown, S., Cairns, M. A., Chambers, J. Q., Eamus, D., ... Yamakura, T. (2005). Tree allometry and improved estimation of carbon stocks and balance in tropical forests. *Oecologia*, 145(1), 87–99. <https://doi.org/10.1007/s00442-005-0100-x>
- Chave, J., Réjou-Méchain, M., Búrquez, A., Chidumayo, E., Colgan, M. S., Delitti, W. B. C., ... Vieilledent, G. (2014). Improved allometric models to estimate the aboveground biomass of tropical trees. *Global Change Biology*, 20(10), 3177–3190. <https://doi.org/10.1111/gcb.12629>
- Clinton, N., Holt, A., Scarborough, J., Yan, L., & Gong, P. (2014). Accuracy Assessment Measures for Object-based Image Segmentation Goodness Accuracy Assessment Measures for Object-based Image Segmentation Goodness. *Photogrammetric Engineering and Remote Sensing*, (November). <https://doi.org/10.14358/PERS.76.3.289>
- Colomina, I., & Molina, P. (2014). ISPRS Journal of Photogrammetry and Remote Sensing Unmanned aerial systems for photogrammetry and remote sensing : A review. *ISPRS Journal of Photogrammetry and Remote Sensing*, 92, 79–97. <https://doi.org/10.1016/j.isprsjprs.2014.02.013>
- Crowley, T. J. (2000). Causes of climate change over the past 1000 years. *Science (New York, N.Y.)*, 289(5477), 270–7. <https://doi.org/10.1126/SCIENCE.289.5477.270>
- Debella-Gilo, M., & Iii, W. (2016). BARE-EARTH EXTRACTION AND DTM GENERATION FROM PHOTOGRAMMETRIC POINT CLOUDS WITH A PARTIAL USE OF AN EXISTING LOWER RESOLUTION DTM. *The International Archives of the Photogrammetry, Remote Sensing and Spatial Information Sciences*, XLI-B3, 201–206. <https://doi.org/10.5194/isprsarchives-XLI-B3-201-2016>

- Definiens. (2009). Definiens eCognition version 8. Retrieved from [http://www.ecognition.com/sites/default/files/eCognition\\_v8\\_Datasheet.pdf](http://www.ecognition.com/sites/default/files/eCognition_v8_Datasheet.pdf)
- Drake, J. B., Dubayah, R. O., Clark, D. B., Knox, R. G., Blair, J. B., Hofton, M. A., ... Prince, S. (2002). Estimation of tropical forest structural characteristics using large-footprint lidar. *Remote Sensing of Environment*, 79(2–3), 305–319. [https://doi.org/10.1016/S0034-4257\(01\)00281-4](https://doi.org/10.1016/S0034-4257(01)00281-4)
- esri. (2011). Lidar Analysis in ArcGIS® 10 for Forestry Applications Lidar Analysis in ArcGIS 10 for Forestry Applications An Esri White Paper. Retrieved February 9, 2018, from <https://www.esri.com/library/whitepapers/pdfs/lidar-analysis-forestry-10.pdf>
- Estornell, J., Ruiz, L. A., Velázquez-Martí, B., & Hermosilla, T. (2011). Analysis of the factors affecting LiDAR DTM accuracy in a steep shrub area. *International Journal of Digital Earth*, 4(6), 521–538. <https://doi.org/10.1080/17538947.2010.533201>
- Ferraz, A., Saatchi, S., Mallet, C., & Meyer, V. (2016). Lidar detection of individual tree size in tropical forests. *Remote Sensing of Environment*, 183, 318–333. <https://doi.org/10.1016/J.RSE.2016.05.028>
- Fritz, A., Kattenborn, T., & Koch, B. (2013). UAV-BASED PHOTOGRAMMETRIC POINT CLOUDS -TREE STEM MAPPING IN OPEN STANDS IN COMPARISON TO TERRESTRIAL LASER SCANNER POINT CLOUDS. *International Archives of the Photogrammetry, Remote Sensing and Spatial Information Sciences*, XL-1/W2. Retrieved from <https://www.int-arch-photogramm-remote-sens-spatial-inf-sci.net/XL-1-W2/141/2013/isprsarchives-XL-1-W2-141-2013.pdf>
- Gallay, M. (2013). GALLAY, M. (2013). Section 2.1.4: Direct Acquisition of Data: Airborne laser scanning. In: Clarke, L.E & Nield, J.M. (Eds.) *Geomorphological Techniques (Online Edition)*. British Society for Geomorphology; London, UK.
- Gerke, M., & Przybilla, H.-J. (2016). Accuracy Analysis of Photogrammetric UAV Image Blocks: Influence of Onboard RTK-GNSS and Cross Flight Patterns. *Photogrammetrie - Fernerkundung - Geoinformation*, 2016(1), 17–30. <https://doi.org/10.1127/pfg/2016/0284>
- Gibbs, H. K., Brown, S., Niles, J. O., & Foley, J. A. (2007). Monitoring and estimating tropical forest carbon stocks: making REDD a reality. *Environmental Research Letters*, 2(4), 45023. <https://doi.org/10.1088/1748-9326/2/4/045023>
- Hyypä, J., Holopainen, M., & Olsson, H. (2012). Laser Scanning in Forests. *Remote Sensing*, 4(12), 2919–2922. <https://doi.org/10.3390/rs4102919>
- IPCC. (2006). IPCC. Retrieved from <https://www.ipcc.ch/meetings/session25/doc4a4b/vol4.pdf>
- Jung, S.-E., Kwak, D.-A., Park, T., Lee, W.-K., & Yoo, S. (2011). Estimating Crown Variables of Individual Trees Using Airborne and Terrestrial Laser Scanners. *Remote Sens*, 3, 2346–2363. <https://doi.org/10.3390/rs3112346>
- Kachamba, D., Ørka, H., Gobakken, T., Eid, T., & Mwase, W. (2016). Biomass Estimation Using 3D Data from Unmanned Aerial Vehicle Imagery in a Tropical Woodland. *Remote Sensing*, 8(11), 968. <https://doi.org/10.3390/rs8110968>
- Kahyani, S., Kahyani, S., Hosseini, S., & Basiri, R. (2011). The Basic of Analytical of Simple Linear Regression in Forestry Studies (Case Study: Relationship Between Basal Area and Tree Coverage of *Quercus brantii* Lindl. In Absardeh, Chahar Mahale and Bakhtiari). *World Applied Sciences Journal*, 14(10), 1599–1606. Retrieved from

<https://pdfs.semanticscholar.org/ac90/5ed60de706da7d198276036a75bcfe3c4bb6.pdf>

- Kershaw, J. A., Ducey, M. J., Beers, T. W., & Husch, B. (2016). *Forest mensuration* (5th ed.). New York: John Wiley . Retrieved from <http://ezproxy.utwente.nl:2200/patron/FullRecord.aspx?p=4731589&echo=1&userid=UKhpPx1CdolYzKF16cOSow%3D%3D&tstamp=1503167854&id=B97043255E1879841CFA59BF3C863D4784523C91>
- Leitold, V., Keller, M., Morton, D. C., Cook, B. D., & Shimabukuro, Y. E. (2015). Airborne lidar-based estimates of tropical forest structure in complex terrain: opportunities and trade-offs for REDD+. *Carbon Balance and Management*, 10(1), 3. <https://doi.org/10.1186/s13021-015-0013-x>
- Lim, Y. S., La, P. H., Park, J. S., Lee, M. H., Pyeon, M. W., & Kim, J.-I. (2015). Calculation of Tree Height and Canopy Crown from Drone Images Using Segmentation. *Journal of the Korean Society of Surveying, Geodesy, Photogrammetry and Cartography*, 33(6), 605–614. <https://doi.org/10.7848/ksgpc.2015.33.6.605>
- Malaysia - Malaysian Meteorological Department. (2017). Retrieved August 7, 2017, from <http://www.met.gov.my/in/web/metmalaysia/climate/generalinformation/malaysia>
- Maltamo, M., Mustonen, K., Hyypä, J., Pitkänen, J., & Yu, X. (2004). The accuracy of estimating individual tree variables with airborne laser scanning in a boreal nature reserve. *Canadian Journal of Forest Research*, 34(9), 1791–1801. <https://doi.org/10.1139/x04-055>
- Maniatis, D., & Mollicone, D. (2010). Options for sampling and stratification for national forest inventories to implement REDD+ under the UNFCCC. *Carbon Balance and Management*, 5:9. <https://doi.org/10.1186/1750-0680-5-9>
- Mesas-Carrascosa, F.-J., Notario García, M., Meroño de Larriva, J., & García-Ferrer, A. (2016). An Analysis of the Influence of Flight Parameters in the Generation of Unmanned Aerial Vehicle (UAV) Orthomosaics to Survey Archaeological Areas. *Sensors*, 16(11), 1838. <https://doi.org/10.3390/s16111838>
- Micheletti, N., Chandler, J. H., & Lane, S. N. (2015). Structure from Motion (SfM) Photogrammetry. *British Society for Geomorphology Geomorphological Techniques*, 2(2). Retrieved from [http://geomorphology.org.uk/sites/default/files/geom\\_tech\\_chapters/2.2.2\\_sfm.pdf](http://geomorphology.org.uk/sites/default/files/geom_tech_chapters/2.2.2_sfm.pdf)
- Mohren, G., Hasenauer, H., Köhl, M., Nabuurs, G., by Ingrid Visseren-Hamakers, E. J., Gupta, A., ... Vijge, M. J. (2012). Forest inventories for carbon change assessments This review comes from a themed issue on Climate systems. *Current Opinion in Environmental Sustainability*, 4, 686–695. <https://doi.org/10.1016/j.cosust.2012.10.002>
- Möller, M., Lymburner, L., & Volk, M. (2007). The comparison index: A tool for assessing the accuracy of image segmentation. *International Journal of Applied Earth Observation and Geoinformation*, 9, 311–321. <https://doi.org/10.1016/j.jag.2006.10.002>
- Næsset, E., Gobakken, T., Holmgren, J., Hyypä, H., Hyypä, J., Maltamo, M., ... Söderman, U. (2004). Laser scanning of forest resources: the nordic experience. *Scandinavian Journal of Forest Research*, 19(6), 482–499. <https://doi.org/10.1080/02827580410019553>
- Nex, F., & Remondino, F. (2013). UAV for 3D mapping applications: a review. <https://doi.org/10.1007/s12518-013-0120-x>

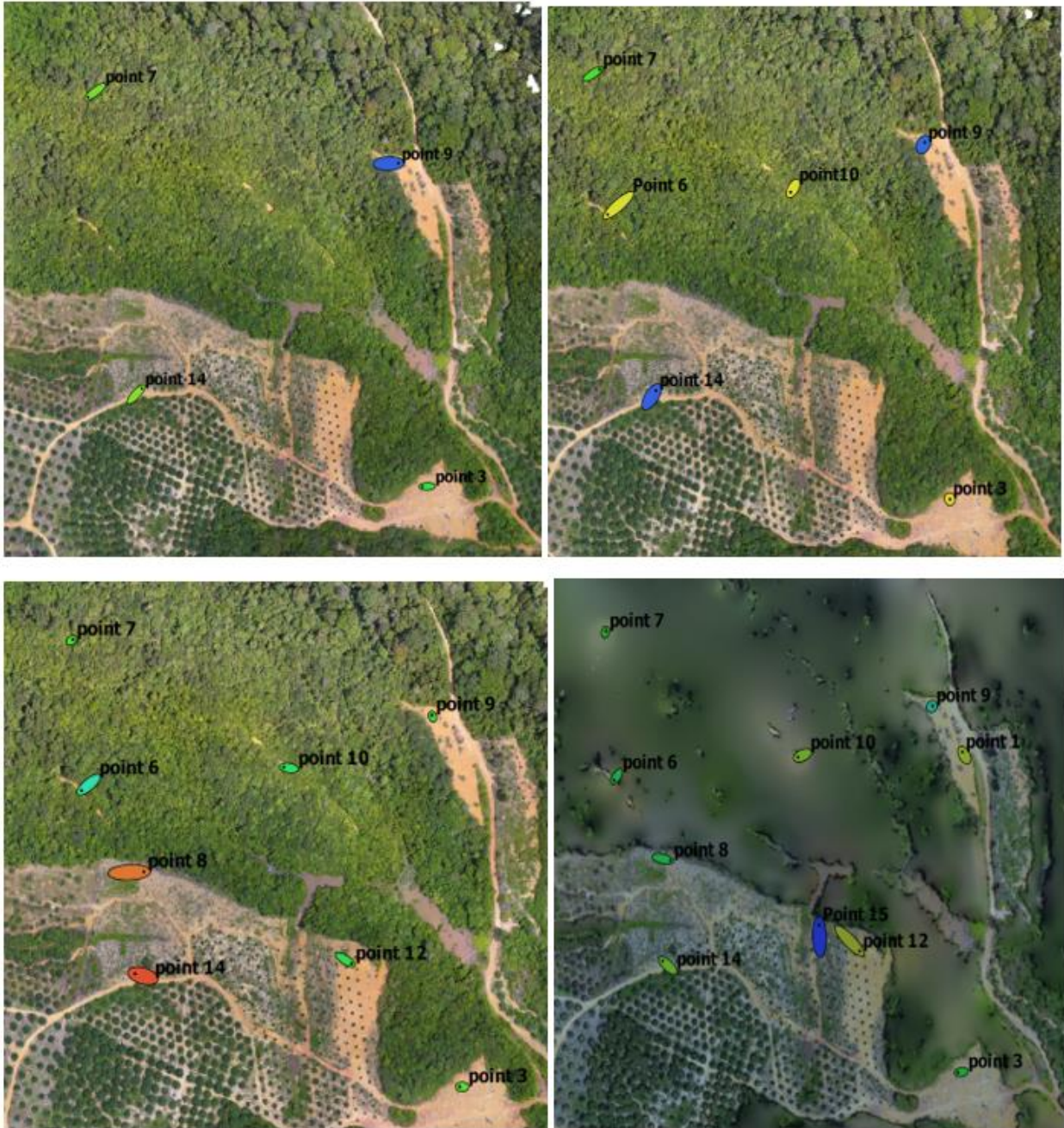
- Niyonsenga, H. (2016). Improving the Accuracy of Uav Image Block Orientation Without Gcps, (February), 76. Retrieved from <https://webapps.itc.utwente.nl/library/2016/msc/gfm/niyonsenga.pdf>
- Omar, H., Hasmadi Ismail, M., & Aziz Hamzah, K. (2015). Estimating Biomass in Logged Tropical Forest Using L-Band SAR (PALSAR) Data and GIS (Penganggaran Biojisim dalam Hutan Tropika telah Diteroka menggunakan Data SAR Berjalur L (PALSAR) dan GIS). *Sains Malaysiana*, 44(8), 1085–1093. Retrieved from [http://www.ukm.my/jsm/pdf\\_files/SM-PDF-44-8-2015/02 Hamidan Omar.pdf](http://www.ukm.my/jsm/pdf_files/SM-PDF-44-8-2015/02 Hamidan Omar.pdf)
- Ordóñez, C., Martínez, J., Arias, P., & Armesto, J. (2010). Measuring building façades with a low-cost close-range photogrammetry system. *Automation in Construction*, 19(6), 742–749. <https://doi.org/10.1016/j.autcon.2010.03.002>
- Ota, T., Ogawa, M., Mizoue, N., Fukumoto, K., & Yoshida, S. (2017). Forest Structure Estimation from a UAV-Based Photogrammetric Point Cloud in Managed Temperate Coniferous Forests. *Forests*, 8(9), 343. <https://doi.org/10.3390/f8090343>
- Ota, T., Ogawa, M., Shimizu, K., Kajisa, T., Mizoue, N., Yoshida, S., ... Ket, N. (2015). Aboveground Biomass Estimation Using Structure from Motion Approach with Aerial Photographs in a Seasonal Tropical Forest. *Forests*, 6(12), 3882–3898. <https://doi.org/10.3390/f6113882>
- Pan, Y., Birdsey, R. A., Fang, J., Houghton, R., Kauppi, P. E., Kurz, W. A., ... Hayes, D. (2011). A Large and Persistent Carbon Sink in the World's Forests. *Science*, 333(6045). Retrieved from <http://science.sciencemag.org/content/333/6045/988.full>
- Paper, C., & Stere, K. (2008). ACCURACY OF CROWN SEGMENTATION AND ESTIMATION OF SELECTED TREES AND FOREST STAND PARAMETERS IN ORDER TO RESOLUTION OF USED DSM AND NDSM MODELS GENERATED FROM DENSE SMALL FOOTPRINT LIDAR DATA. In *The international Archives of The photogrammetry, Remote sensing and Spatial Information Sciences* (Vol. XXXVIII\_ B, pp. 27–33).
- Pirotti, F. (2011). Analysis of full-waveform LiDAR data for forestry applications: A review of investigations and methods. *IForest*, 4(JUNE), 100–106. <https://doi.org/10.3832/ifor0562-004>
- Popescu, S. C., Wynne, R. H., & Nelson, R. F. (2002). Estimating plot-level tree heights with lidar: local filtering with a canopy-height based variable window size. *Computers and Electronics in Agriculture*, 37(1–3), 71–95. [https://doi.org/10.1016/S0168-1699\(02\)00121-7](https://doi.org/10.1016/S0168-1699(02)00121-7)
- REDD+. (2012). *REDD plus HOW TO MEASURE AND MONITOR FOREST CARBON*. Retrieved from [https://www.ffpri.affrc.go.jp/redd-rdc/en/reference/cookbook/redd\\_cookbook\\_all\\_high\\_en.pdf](https://www.ffpri.affrc.go.jp/redd-rdc/en/reference/cookbook/redd_cookbook_all_high_en.pdf)
- Reuben, J., Hussin, Y. A., & Kloosterman, D. E. H. (2017). ACCURACY OF TREE HEIGHT DERIVED FROM POINT CLOUDS OF UAV COMPARED TO AIRBORNE LIDAR AND ITS EFFECT ON ESTIMATING BIOMASS AND CARBON STOCK IN PART OF TROPICAL FOREST IN MALAYSIA. *Unpublished Msc Thesis*. Retrieved from <https://ezproxy.utwente.nl:2315/library/2017/msc/nrm/hongoa.pdf>
- Spetsakis, M., & Aloimonos, J. Y. (1991). A multi-frame approach to visual motion perception. *International Journal of Computer Vision*, 6(3), 245–255. <https://doi.org/10.1007/BF00115698>
- Tahar, K. N. (2013). AN EVALUATION ON DIFFERENT NUMBER OF GROUND CONTROL POINTS IN UNMANNED AERIAL VEHICLE PHOTOGRAMMETRIC BLOCK. In *ISPRS 8th 3DGeoInfo Conference & WG II/2 Workshop* (Vol. XL-2/W2). Istanbul, Turkey: International Archives of the Photogrammetry,



- Remote Sensing and Spatial Information Sciences. Retrieved from <https://pdfs.semanticscholar.org/5c29/6571cdd70cc5a04569447fd3dcdf72300204.pdf>
- Torres-Sánchez, J., López-Granados, F., Serrano, N., Arquero, O., Peña, J. M., & Addink, E. (2015). High-Throughput 3-D Monitoring of Agricultural-Tree Plantations with Unmanned Aerial Vehicle (UAV) Technology. *PLOS ONE*, *10*(6), e0130479. <https://doi.org/10.1371/journal.pone.0130479>
- UNFCCC. (1997). Kyoto Protocol to the United Nations framework Convention on Climate change. Retrieved May 31, 2017, from [http://unfccc.int/kyoto\\_protocol/items/2830.php](http://unfccc.int/kyoto_protocol/items/2830.php)
- UNFCCC. (2010). *Report of the Conference of the Parties on its sixteenth session*. Cancun . Retrieved from <https://unfccc.int/resource/docs/2010/cop16/eng/07a01.pdf>
- Unmanned Aerial Vehicle Systems Association Advantages of UAVs. (2017). Retrieved May 3, 2017, from <https://www.uavs.org/advantages>
- US Department of Commerce, NOAA, E. S. R. L. (2017). ESRL Global Monitoring Division - Global Greenhouse Gas Reference Network. Retrieved December 21, 2017, from <https://www.esrl.noaa.gov/gmd/ccgg/trends/global.html>
- Wallace, L., Lucieer, A., Malenovsky, Z., Turner, D., & Vopěnka, P. (2016). Assessment of Forest Structure Using Two UAV Techniques: A Comparison of Airborne Laser Scanning and Structure from Motion (SfM) Point Clouds. *Forests*, *7*(3), 62. <https://doi.org/10.3390/f7030062>
- Wehr, A., & Lohr, U. (1999). Airborne laser scanning—an introduction and overview. *ISPRS Journal of Photogrammetry & Remote Sensing*, *54*, 68–82. Retrieved from [http://knightlab.org/rsc/readings/airborne\\_laser\\_scanning.pdf](http://knightlab.org/rsc/readings/airborne_laser_scanning.pdf)
- Westoby, M. J., Brasington, J., Glasser, N. F., Hambrey, M. J., & Reynolds, J. M. (2012). “Structure-from-Motion” photogrammetry: A low-cost, effective tool for geoscience applications. *Geomorphology*, *179*, 300–314. <https://doi.org/10.1016/j.geomorph.2012.08.021>
- WWF. (2017). The Malaysian Rainforest | WWF Malaysia. Retrieved July 26, 2017, from [http://www.wwf.org.my/about\\_wwf/what\\_we\\_do/forests\\_main/the\\_malaysian\\_rainforest/](http://www.wwf.org.my/about_wwf/what_we_do/forests_main/the_malaysian_rainforest/)
- Yao, W., Krull, J., Krzystek, P., & Heurich, M. (2014). Sensitivity Analysis of 3D Individual Tree Detection from LiDAR Point Clouds of Temperate Forests. *Forests*, *5*(6), 1122–1142. <https://doi.org/10.3390/f5061122>
- Zarco-Tejada, P. J., Diaz-Varela, R., Angileri, V., & Loudjani, P. (2014). Tree height quantification using very high resolution imagery acquired from an unmanned aerial vehicle (UAV) and automatic 3D photo-reconstruction methods. *European Journal of Agronomy*, *55*, 89–99. <https://doi.org/10.1016/j.eja.2014.01.004>
- Zolkos, S. G., Goetz, S. J., & Dubayah, R. (2013). A meta-analysis of terrestrial aboveground biomass estimation using lidar remote sensing. *Remote Sensing of Environment*, *128*, 289–298. <https://doi.org/10.1016/j.rse.2012.10.017>



Appendix 2 Configuration of GCPs for UAV DTM 4,6,8 and 10.



Appendix 3 t-test to compare height for ALS and UAV DTM's using 500 points.

	<i>ALS DTM</i>	<i>UAV DTM4</i>	<i>ALS DTM</i>	<i>UAV DTM 6</i>	<i>ALS DTM</i>	<i>UAV DTM8</i>	<i>ALS DTM</i>	<i>UAV DTM 10</i>
Mean	56.80	55.66	56.80	55.49	56.80	55.54	56.80	55.50
Variance	50.49	39.83	50.49	39.81	50.49	37.69	50.49	37.42
Observations	500	500	500	500	500	500	500	500
df	998.00		998		998		998	
t Stat	2.69		3.08		3.00		3.10	
P(T<=t) one-tail	0.00		0.00		0.00		0.00	
t Critical one-tail	1.65		1.65		1.65		1.65	
P(T<=t) two-tail	0.01		0.00		0.00		0.00	
t Critical two-tail	1.96		1.96		1.96		1.96	

Appendix 4 t-test to compare height for ALS and UAV DTMs in closed space

t-Test: Two-Sample Assuming Equal Variances

	<i>ALS DTM</i>	<i>DTM4</i>	<i>ALS DTM</i>	<i>DTM 6</i>	<i>DTM8</i>	<i>ALS DTM</i>	<i>DTM 10</i>
Mean	57.62555	55.48135	57.62555	55.35874618	55.39161	57.62555	55.33107
Variance	51.03796	42.23877	51.03796	41.81874939	38.72133	51.03796	38.30909
Observations	324	324	324	324	324	324	324
df	646		646			646	
t Stat	3.996228		4.234276			4.369332	
P(T<=t) one-tail	3.59E-05		1.31E-05			7.26E-06	
t Critical one-tail	1.647216		1.647216			1.647216	
P(T<=t) two-tail	7.18E-05		2.63E-05			1.45E-05	
			1.963643			1.963643	

Appendix 5 F-test to compare tree height for ALS and UAV tree heights in closer altitude.

F-Test Two-Sample for Variances

	<i>UAV tree height</i>	<i>ALS tree height</i>
Mean	15.53644	14.5093
Variance	41.70708	34.62624
Observations	154	154
df	153	153
F	1.204494	
P(F<=f) one-tail	0.125483	
F Critical one-tail	1.30576	

Appendix 6 matched trees for comparison of UAV and ALS CHM.

Tree_No	Latitude	longtiude	DBH_cm	ALS_Tree height	UAV_Tree height
1	3.728245000	102.9497725	14.9	11.90	10.40
7	3.728175278	102.9497672	23.2	5.70	11.03
15	3.728281389	102.9496244	13.3	5.09	10.62
16	3.728290556	102.9497578	12.0	12.45	14.50
18	3.728371111	102.9497244	12.0	11.35	10.66
19	3.728337500	102.9497372	9.0	12.64	13.70
24	3.728410278	102.9497394	11.2	10.17	10.65
27	3.728419444	102.9498308	17.0	8.16	10.34
28	3.728323889	102.9500000	6.4	8.37	12.07
29	3.728333889	102.9500000	15.5	6.13	10.23
30	3.728371944	102.9498342	17.5	6.99	9.58
31	3.728341944	102.9498572	6.1	5.52	9.30
34	3.728352222	102.9498100	9.5	4.69	9.71
35	3.728352500	102.9498267	6.5	7.89	8.79
38	3.728295000	102.9498228	9.2	13.14	13.84
41	3.728290278	102.9500000	5.7	4.93	9.32
44	3.728351389	102.9500000	6.3	13.11	12.05
45	3.728298333	102.9500000	16.5	5.64	9.25
50	3.728248611	102.9500000	7.5	7.38	10.25
53	3.728265278	102.9500000	7.1	9.16	10.79
56	3.728225556	102.9498514	9.5	7.22	9.50
60	3.728293889	102.9498389	10.5	5.26	9.02
61	3.728223056	102.9500000	7.6	5.64	9.25
62	3.728247778	102.9498069	6.5	8.94	10.01
72	3.727966944	102.9503081	6.2	7.30	9.92
77	3.728184722	102.9502917	5.1	8.46	12.51
79	3.728209722	102.9503250	5.5	4.79	12.06

80	3.728209722	102.9503044	8.8	4.79	12.06
81	3.728202778	102.9502717	12.5	7.03	12.46
87	3.728212778	102.9502858	6.5	5.56	12.53
88	3.728278889	102.9503022	8.0	6.19	10.45
89	3.728228333	102.9503006	8.8	5.85	9.19
90	3.728231389	102.9503681	10.2	5.50	9.04
91	3.728287778	102.9503175	5.3	8.44	12.20
92	3.728267222	102.9502622	7.5	7.25	10.41
96	3.728282778	102.9502583	7.1	7.39	9.11
97	3.728282778	102.9502481	6.9	5.07	9.25
103	3.728198056	102.9502289	6.9	8.69	13.64
104	3.728150278	102.9501744	9.3	6.18	10.60
105	3.728152500	102.9501769	7.6	5.56	9.97
106	3.728184167	102.9501861	9.4	7.66	11.44
107	3.728152222	102.9501861	10.6	4.58	9.79
118	3.728098889	102.9502233	16.0	8.50	12.08
121	3.728074167	102.9502614	7.3	8.35	12.22
122	3.728075833	102.9502758	12.0	8.89	12.12
126	3.728020833	102.9502472	6.0	5.83	10.43
127	3.728190000	102.9502233	7.3	8.69	13.64
128	3.728131944	102.9502233	7.1	9.39	11.53
129	3.728131944	102.9502500	6.0	8.46	12.51
130	3.728121944	102.9503011	14.5	8.42	11.94
131	3.728161667	102.9503011	9.9	5.27	10.39
133	3.728188611	102.9503453	10.2	5.48	10.59
134	3.728169722	102.9503408	12.0	5.48	10.59
135	3.728152500	102.9503303	10.5	8.42	11.94
137	3.728125278	102.9503889	15.0	6.52	10.16
140	3.728197222	102.9504467	9.5	15.14	15.99
144	3.728158889	102.9503692	5.3	8.42	11.94
145	3.728211389	102.9503692	7.4	5.23	9.66
146	3.728211389	102.9504075	14.4	9.52	12.07
147	3.728189722	102.9503939	13.5	12.87	15.78
153	3.728014722	102.9505375	6.1	6.14	10.23
154	3.728047500	102.9506028	8.2	5.28	9.52
155	3.727965556	102.9507036	10.7	8.39	15.44
157	3.727977222	102.9507072	6.5	8.87	15.61
158	3.728058056	102.9506319	8.2	12.83	18.12
160	3.728021944	102.9506769	14.0	6.79	13.30
161	3.728099167	102.9505600	8.3	17.66	19.94
164	3.728077222	102.9506011	30.0	12.83	18.12
165	3.728062500	102.9505642	8.0	15.93	16.92
167	3.728042222	102.9506506	6.0	6.89	11.97
169	3.728113889	102.9505811	11.5	14.69	17.66
170	3.728124722	102.9507811	8.0	13.54	16.65

171	3.728023056	102.9504533	8.0	7.80	9.03
179	3.727995556	102.9504875	7.0	8.58	11.12
180	3.727962500	102.9505542	9.4	7.40	12.65
181	3.727954444	102.9505425	11.0	8.78	11.40
185	3.728042222	102.9506956	11.0	7.00	13.84
196	3.728042778	102.9506744	14.0	12.69	13.99
197	3.728036111	102.9507061	14.0	5.97	14.06
198	3.727992222	102.9506844	12.3	8.87	15.61
199	3.727961944	102.9506594	15.0	10.04	11.52
202	3.727977778	102.9506647	16.7	6.26	12.45
203	3.727993611	102.9506286	8.3	9.29	12.64
205	3.727933611	102.9506064	7.6	8.19	11.56
207	3.729873333	102.9500658	17.0	10.77	16.66
210	3.729636389	102.9500000	14.0	19.69	21.96
211	3.729660000	102.9500061	7.6	14.61	21.54
216	3.729637500	102.9500547	9.6	15.32	23.12
217	3.729649167	102.9500472	6.0	16.36	21.08
218	3.729655556	102.9500686	5.5	13.93	23.23
220	3.729651667	102.9500519	30.5	16.39	20.10
221	3.729670000	102.9500000	14.2	19.63	23.20
225	3.729671389	102.9500000	10.1	16.02	20.51
228	3.729756944	102.9500500	26.5	18.81	18.99
231	3.729784722	102.9501586	9.5	10.02	12.57
232	3.729536667	102.9503772	35.0	11.92	20.22
241	3.729474444	102.9502853	12.5	11.05	19.33
242	3.729428889	102.9502364	8.5	13.33	20.68
249	3.729308056	102.9502544	31.5	13.94	22.85
252	3.729378333	102.9501881	10.7	12.11	20.72
256	3.729362500	102.9503022	12.0	13.24	21.81
263	3.729500833	102.9504575	9.0	16.92	23.66
264	3.729456944	102.9504872	14.2	14.13	20.39
265	3.729446944	102.9505217	29.1	7.05	14.92
274	3.726534722	102.9520700	19.5	8.69	10.15
275	3.726620000	102.9520778	21.4	6.00	10.13
276	3.726593611	102.9521467	13.5	7.09	9.16
279	3.726486667	102.9520256	11.8	5.44	8.25
283	3.726561667	102.9519939	11.0	6.49	9.33
286	3.726481944	102.9520342	12.0	7.65	10.27
292	3.726422500	102.9520283	11.9	5.50	8.24
297	3.726371389	102.9520708	18.0	12.11	10.58
308	3.726353611	102.9520794	13.5	6.72	8.24
310	3.727585556	102.9519578	12.6	9.05	14.48
311	3.727559444	102.9519881	11.0	9.94	14.68
312	3.727592222	102.9520217	7.0	12.42	14.13
313	3.727555833	102.9520453	6.8	12.42	14.13



314	3.727579167	102.9520397	6.9	8.04	12.72
315	3.727614167	102.9520289	39.2	9.12	13.58
316	3.727658333	102.9520442	10.2	8.36	14.19
317	3.727596111	102.9519692	19.5	7.12	11.96
323	3.727626944	102.9520425	15.0	7.18	13.50
324	3.727602500	102.9519839	8.0	9.10	14.52
326	3.727571944	102.9520269	8.0	6.10	11.83
327	3.727530278	102.9520514	10.0	6.15	12.77
328	3.727518056	102.9520031	14.1	6.41	12.16
331	3.727506944	102.9519922	15.5	8.73	12.72
333	3.727515833	102.9519664	9.6	10.77	11.49
334	3.727553056	102.9519422	5.0	9.77	14.09
335	3.727553056	102.9519422	7.2	9.77	14.09
336	3.727681111	102.9521003	15.0	6.66	12.40
337	3.727681111	102.9521003	7.0	9.78	12.06
338	3.727664444	102.9520944	6.0	5.11	12.04
339	3.727654167	102.9520878	11.0	7.07	11.93
340	3.727647778	102.9520739	19.7	11.17	14.69
341	3.727647778	102.9520739	22.3	8.36	14.19
343	3.727573889	102.9521275	17.1	10.91	15.87
344	3.727588611	102.9521331	12.5	18.04	20.57
347	3.727623056	102.9520039	13.2	8.68	13.19
350	3.728214167	102.9496172	8.6	12.70	14.17
351	3.728214167	102.9496172	15.1	12.70	14.17
356	3.728259444	102.9496003	16.7	7.83	13.40
357	3.728202500	102.9495867	11.0	12.76	13.32
365	3.728196389	102.9496694	15.0	12.96	11.78
369	3.728204167	102.9497167	11.5	14.00	16.79
372	3.728286111	102.9496700	9.8	7.26	10.41
373	3.728289167	102.9496406	22.5	6.64	10.68
378	3.728344444	102.9496242	14.0	5.89	10.28
380	3.728363611	102.9495236	13.8	7.30	13.62
381	3.728310000	102.9495608	8.2	8.86	14.43
383	3.728305556	102.9495331	6.2	9.06	14.47
384	3.728259722	102.9495544	12.5	9.27	12.80
385	3.728256111	102.9495322	10.4	8.39	13.68
411	3.729087778	102.9491681	10.0	11.64	12.62
412	3.728945000	102.9494325	15.3	9.93	13.50
413	3.728945000	102.9494325	5.2	9.93	13.50
414	3.728945000	102.9494325	10.5	9.93	13.50
439	3.729662778	102.9493967	12.1	7.32	11.88
440	3.729542222	102.9494883	8.9	10.22	13.31
441	3.729640278	102.9492169	8.2	8.54	13.65
442	3.729541667	102.9494889	18.3	10.22	13.31
443	3.729570278	102.9494811	7.6	6.85	11.50

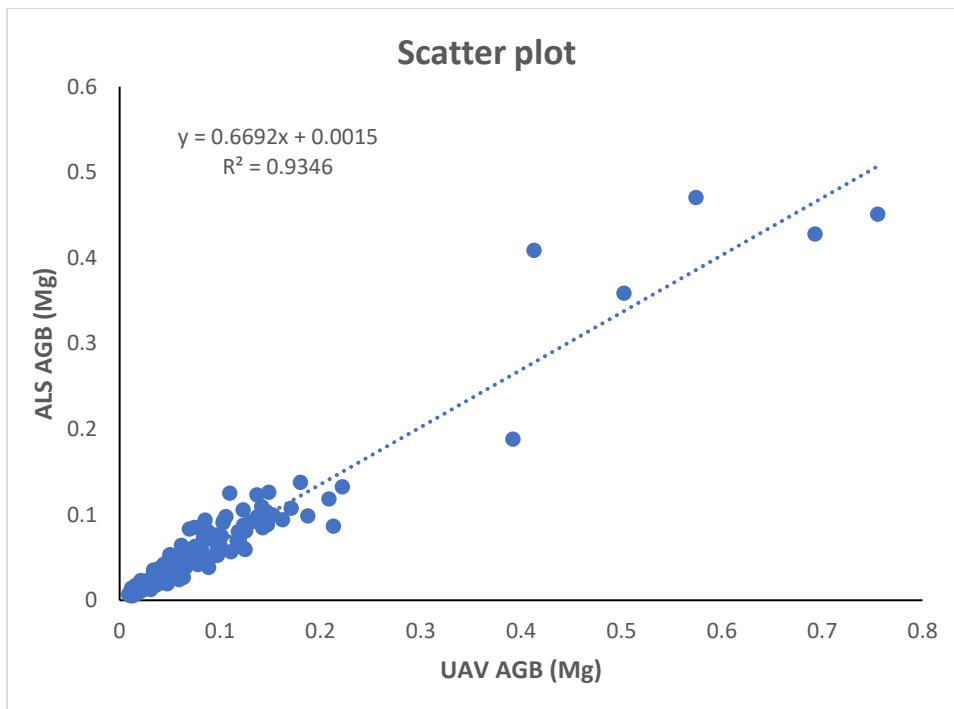
444	3.729733611	102.9494261	10.1	10.59	10.08
445	3.729584722	102.9494408	17.6	9.83	10.66
446	3.729661389	102.9494753	10.8	7.12	11.81
447	3.729650278	102.9495211	11.6	8.62	12.51
448	3.729684444	102.9495025	9.0	7.72	10.97
449	3.729650556	102.9494889	18.8	7.45	12.68
450	3.729650556	102.9494889	17.0	7.45	12.68
451	3.729630000	102.9494431	9.4	10.70	13.98
452	3.729557500	102.9494025	17.1	6.41	13.27
453	3.729610556	102.9493783	12.8	12.04	11.60
455	3.729639444	102.9493758	8.7	6.95	12.08
459	3.729465278	102.9493922	12.1	10.81	10.85
462	3.729678889	102.9493475	7.9	11.15	10.09
463	3.729694167	102.9492703	10.5	6.75	11.67
465	3.729698889	102.9492417	12.4	9.53	12.71
466	3.729698889	102.9492417	8.0	9.53	12.71
468	3.729645000	102.9492853	12.5	9.61	12.53
471	3.729638056	102.9493675	13.9	13.36	11.12
474	3.729631667	102.9492686	6.2	5.75	12.45
476	3.729521111	102.9493869	6.1	11.26	9.50
486	3.728209722	102.9503250	23.7	4.79	12.06
487	3.728209722	102.9503044	12.3	4.79	12.06
488	3.728202778	102.9502717	11.7	7.03	12.46
496	3.728228333	102.9503006	10.8	5.85	9.19
497	3.728231389	102.9503681	17.0	5.50	9.04
498	3.728287778	102.9503175	5.8	8.44	12.20
502	3.728269444	102.9502583	13.0	4.77	11.57
503	3.728282778	102.9502583	11.0	7.39	9.11
510	3.728198056	102.9502289	10.0	8.69	13.64
511	3.728150278	102.9501744	13.7	6.18	10.60
512	3.728152500	102.9501769	21.4	6.40	11.20
513	3.728184167	102.9501861	18.0	7.66	11.44
514	3.728152222	102.9501861	20.0	4.58	9.79
525	3.728098889	102.9502233	16.0	8.50	12.08
533	3.728020833	102.9502472	25.2	5.83	10.43
534	3.728190000	102.9502233	17.0	8.69	13.64
536	3.728131944	102.9502500	8.0	8.46	12.51
537	3.728121944	102.9503011	19.0	8.42	11.94
538	3.728161667	102.9503011	16.0	5.27	10.39
540	3.728188611	102.9503453	8.0	5.48	10.59
541	3.728169722	102.9503408	8.0	5.48	10.59
542	3.728152500	102.9503303	18.0	8.42	11.94
543	3.728072222	102.9503353	5.0	8.12	10.37
544	3.728125278	102.9503889	15.0	6.52	10.16
545	3.728188611	102.9503972	7.5	12.87	15.78

551	3.728158889	102.9503692	19.6	8.42	11.94
552	3.728211389	102.9503692	12.0	5.23	9.66
553	3.728211389	102.9504075	10.0	9.52	12.07
554	3.728189722	102.9503939	8.0	12.87	15.78
555	3.728209722	102.9503250	11.0	4.79	12.06

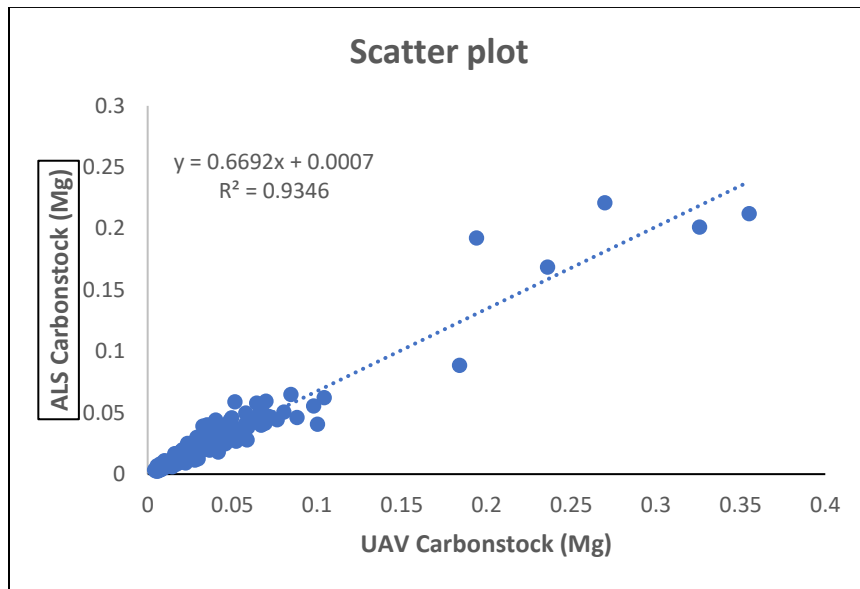
Appendix 7 Comparison of UAV ALS CHM in controlled experiment..

statistics	
R <sup>2</sup>	0.6
RMSE	5.1
RMSE%	16.75

Appendix 8 Relationship between ALS and UAV biomass.



Appendix 9 Relationship between ALS and UAV carbon stock.



Appendix 10 F-test to compare ALS and UAV AGB.

	<i>ALS AGB</i>	<i>UAV AGB</i>
Mean Biomass (Mg) per tree	0.049	0.054
Variance	0.004	0.005
Observations	30	30
df	29	29
F	0.774	
P(F<=f) one-tail	0.247	
F Critical one-tail	0.537	